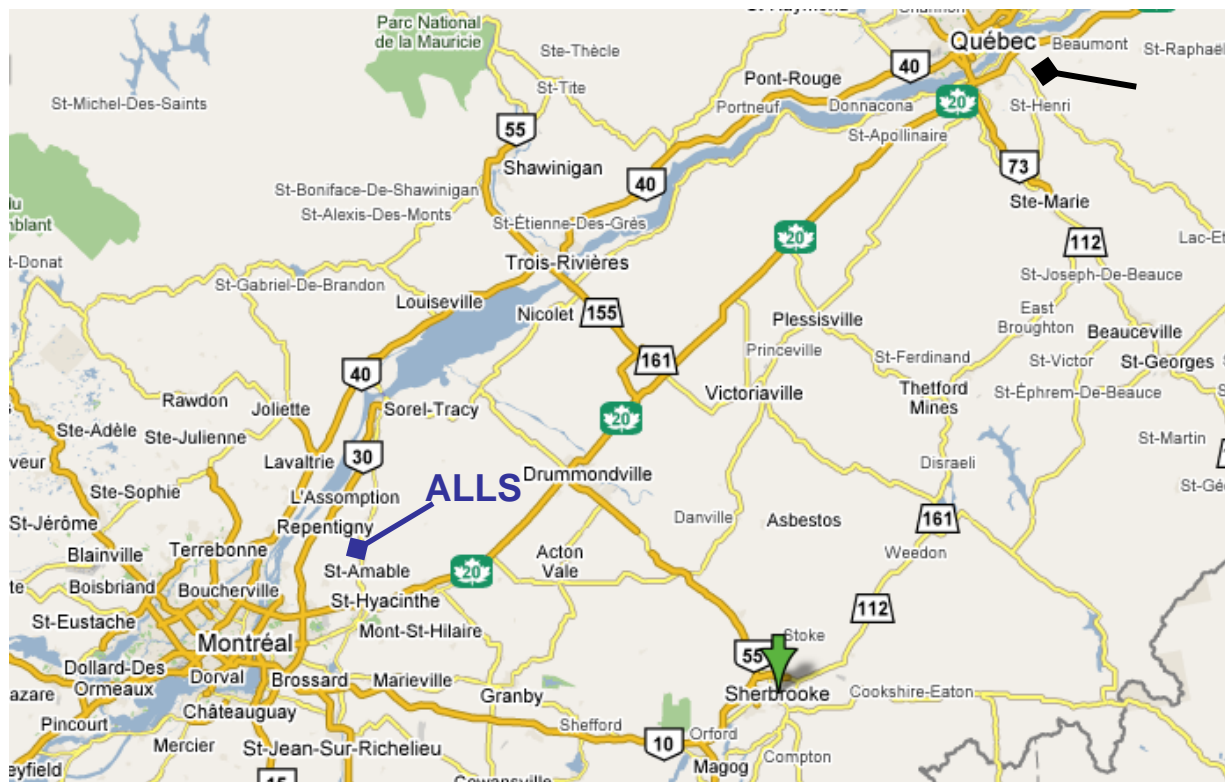


# “Molecules in Intense Laser Fields – Femto to Attosecond Dynamics”

and / or

## “FAST-Femto-Attosecond Simulation (Science) & Theory (Technology)”



NRC

(Ottawa)

ALLS

Québec

Sherbrooke

André D. Bandrauk, PhD, FRSC, FAAAS

Canada Research Chair

Computational Chemistry & Molecular Photonics

Université de Sherbrooke

Potential energy :  $V_o : \frac{e^2}{a_o} = 1 \text{ Hartree} = 27.2 \text{ eV},$  (1)

Electric field  $E_o : \frac{e}{a_o} = 5 \times 10^9 \text{ V/cm},$  (2)

Intensity  $I_o = cE_o^2 / 8\pi = 3.5 \times 10^{16} \text{ W/cm}^2,$  (3)

Distance  $a_o = 0.0529 \text{ nm},$  (4)

Time  $t_o = 24.2 \text{ as}.$  (5)

**Table I**

**Evolution of Laser Parameters [1]**

| Time (s)                       |                   | Intensity (Watts/cm <sup>2</sup> ) |                   | Year |
|--------------------------------|-------------------|------------------------------------|-------------------|------|
| Nano                           | 10 <sup>-9</sup>  | Giga                               | 10 <sup>+9</sup>  | 1980 |
| Pico                           | 10 <sup>-12</sup> | Tera                               | 10 <sup>+12</sup> | 1985 |
| SERS                           |                   |                                    |                   |      |
| Femto                          | 10 <sup>-15</sup> | Peta                               | 10 <sup>+15</sup> | 1990 |
| 1 a.u : 24 x 10 <sup>-18</sup> |                   | $I_o = 3.5 \times 10^{+16}$        |                   |      |
| Atto                           | 10 <sup>-18</sup> | Exa                                | 10 <sup>+18</sup> | 2005 |
| Zepto                          | 10 <sup>-21</sup> | Zetta                              | 10 <sup>+21</sup> | 2009 |
| Yocto                          | 10 <sup>-24</sup> | Yotta                              | 10 <sup>+24</sup> | ?    |

10<sup>29</sup>  
to field  
(1-3), 1

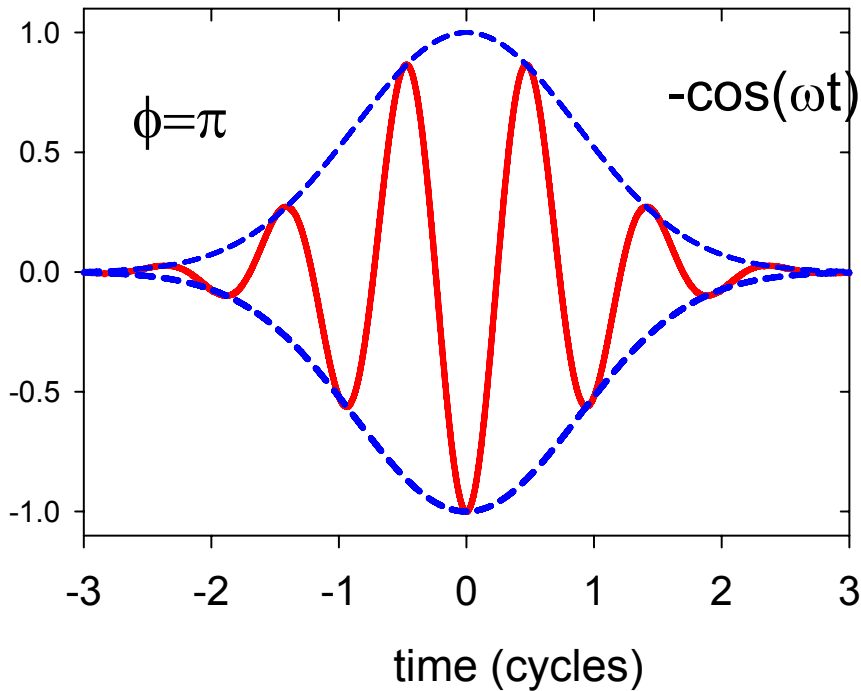
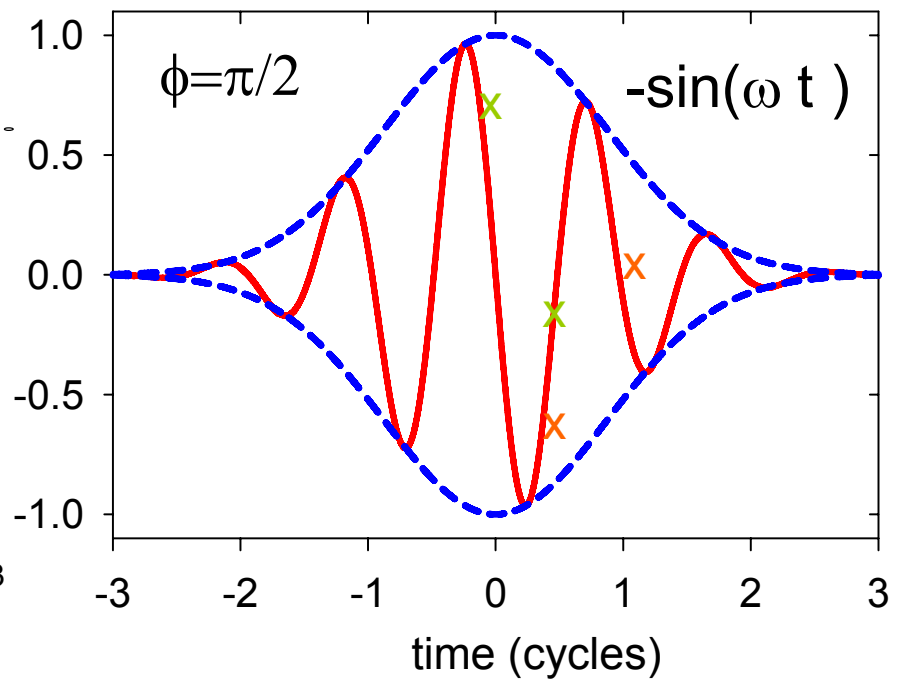
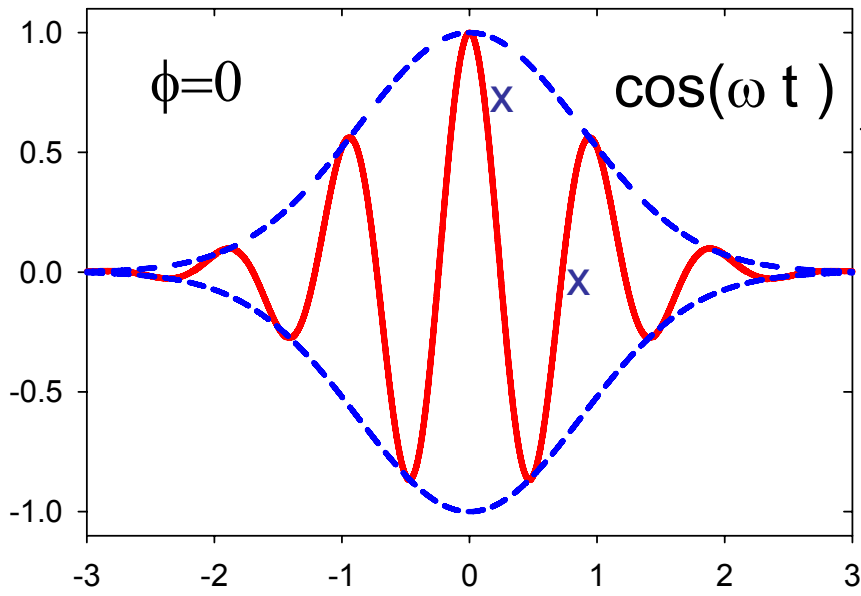
nd  
ns  
ate

representation these radiatively induced distortions creating LIMP's as discussed above lead to *bond softening* via laser-induced avoided crossing of molecular potentials [26-27]. At such intensities, one needs to consider further ionization and the remaining molecular ion potentials become LIMP's in the presence of intense laser pulses. The molecular ions, bound or dissociative can also undergo Above Threshold Dissociation, ATD, [20], [26-27].

Schwinger limit ~ 10\*\*29 W/cm2)

Sunlight: 0.12 W/cm2

electric field  $E(t) / E_0$  and its envelope



1 cycle = 2.66 fs  
for  $\lambda = 800$  nm

$$E(t) = \varepsilon_0(t) \cos(\omega t + \Phi)$$

F Krausz, Science 305,1267(2004)

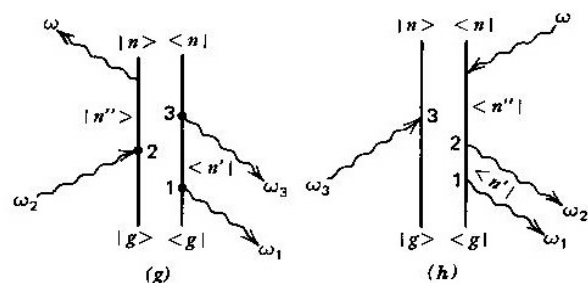
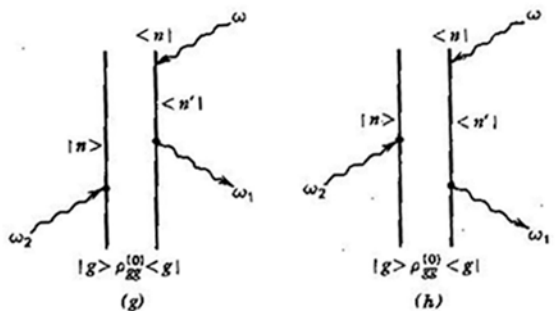
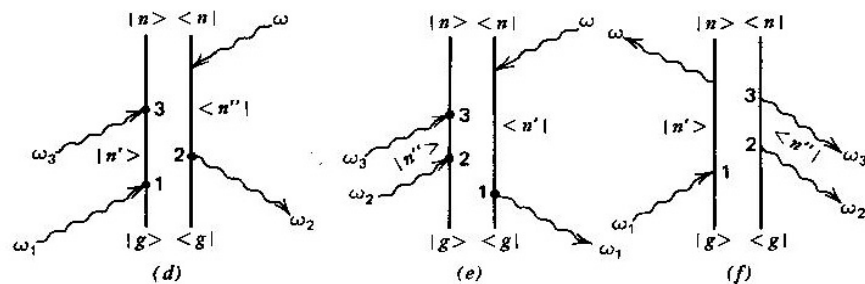
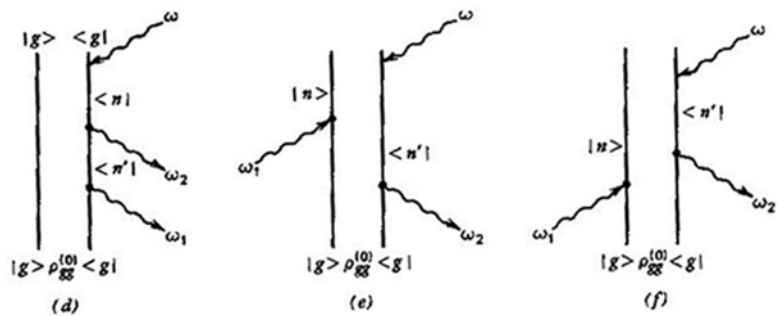
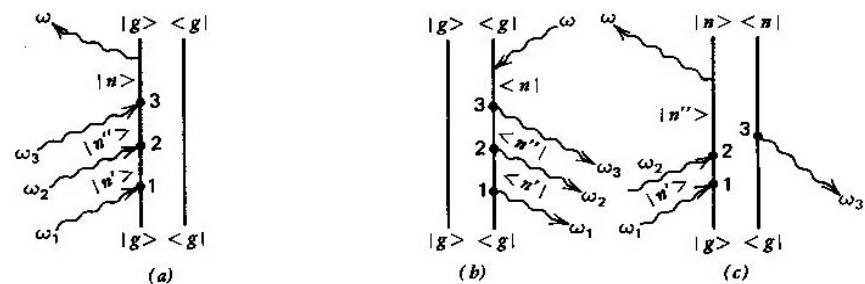
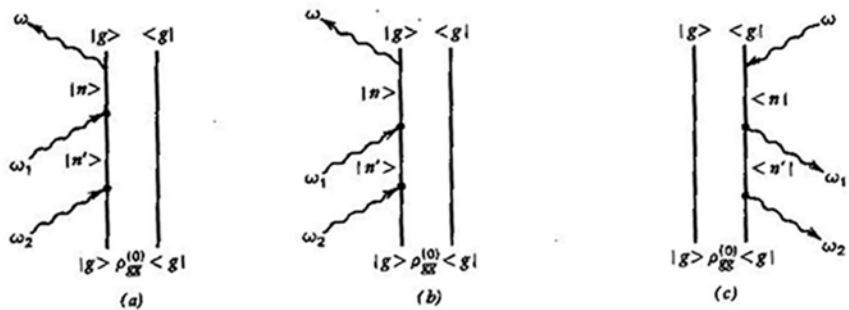


Fig. 2.2 The complete set of eight diagrams for the eight terms in  $\rho^{(2)}$  ( $\omega = \omega_1 + \omega_2$ ).

Fig. 2.3 The eight basic diagrams for  $\rho^{(3)}$  ( $\omega = \omega_1 + \omega_2 + \omega_3$ ).

# MAXWELL – SCHROEDINGER

MAXWELL

Classical      Quantum

$$\frac{\partial^2 E}{\partial z^2} - \frac{1}{c^2} \frac{\partial^2 E}{\partial t^2} = \frac{4\pi}{c^2} \frac{\partial^2 P}{\partial t^2}$$

$P = \text{Medium Polarization} = P(E)$

(1<sup>st</sup> Order  $P = \alpha E$ )

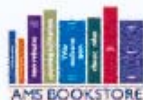
SCHROEDINGER

$$i\hbar \frac{\partial |\psi\rangle}{\partial t} = (\hat{H}_0 + \hat{V}(t)) |\psi\rangle$$

$$P = P(E) = n_0 \langle \psi | \hat{\mu}_0 | \psi \rangle$$

$$|\psi\rangle = \sum_j c_j e^{iE_j t/\hbar} |\Psi_j\rangle$$

$$V_{ii} = -P_{ii} (e(z,t) \cos(kz - \omega t))$$



# AMERICAN MATHEMATICAL SOCIETY

[NEW TITLES](#)
[FAQ](#)
[KEEP INFORMED](#)
[REVIEW CART](#)
[CONTACT US](#)


[\(Advanced Search\)](#)
[Browse by Subject](#)


[Return to List](#)

## High-Dimensional Partial Differential Equations in Science and Engineering

Edited by: **André Bandrauk**, *Université de Sherbrooke, QC, Canada*, **Michel C. Delfour**, *Université de Montréal, QC, Canada*, and **Claude Le Bris**, *École Nationale des Ponts et Chaussées, Marne La Vallée, France*, and *INRIA Rocquencourt, Le Chesnay, France*

[Table of Contents](#)


**CRM Proceedings & Lecture Notes**  
2007; 194 pp; softcover  
Volume: 41  
ISBN-10: 0-8218-3853-9  
ISBN-13: 978-0-8218-3853-2  
**List Price: US\$79**  
Member Price: **US\$63**  
Order Code: CRMP/41

**Not yet published.**  
Expected publication date is July 14, 2007.

[Suggest to a Colleague](#)


High-dimensional spatio-temporal partial differential equations are a major challenge to scientific computing of the future. Up to now deemed prohibitive, they have recently become manageable by combining recent developments in numerical techniques, appropriate computer implementations, and the use of computers with parallel and even massively parallel architectures. This opens new perspectives in many fields of applications. Kinetic plasma physics equations, the many body Schrödinger equation, Dirac and Maxwell equations for molecular electronic structures and nuclear dynamic computations, options pricing equations in mathematical finance, as well as Fokker-Planck and fluid dynamics equations for complex fluids, are examples of equations that can now be handled.

The objective of this volume is to bring together contributions by experts of international stature in that broad spectrum of areas to confront their approaches and possibly bring out common problem formulations and research directions in the numerical solutions of high-dimensional partial differential equations in various fields of science and engineering with special emphasis on chemistry and physics.

Titles in this series are co-published with the Centre de Recherches Mathématiques.

### Readership

Graduate students and research mathematicians interested in numerical solutions of high-dimensional PDE's.



Available online at [www.sciencedirect.com](http://www.sciencedirect.com)

SCIENCE @ DIRECT®

Chemical Physics Letters 419 (2006) 346–350

CHEMICAL  
PHYSICS  
LETTERS

[www.elsevier.com/locate/cplett](http://www.elsevier.com/locate/cplett)

# Complex integration steps in decomposition of quantum exponential evolution operators

André D. Bandrauk<sup>1</sup>, Effat Dehghanian<sup>\*</sup>, Huizhong Lu

*Laboratoire de Chimie Théorique, Faculté des Sciences, Université de Sherbrooke, Qué., Canada J1K 2R1*

Received 28 October 2005; in final form 1 December 2005

Available online 22 December 2005

---

## Abstract

We generalize previous high-order exponential split operator methods for solving time-dependent Schrödinger equations [A.D. Bandrauk, H. Shen, Chem. Phys. Lett. 176 (1991) 428] by introducing complex integration steps ( $a + ib$ ) with real positive part  $a$ . We show that this new procedure avoids real negative steps which occur generally in high-order split operator methods. New highly accurate splitting schemes are thus derived and the efficiency of these is demonstrated in the calculation of the eigenstates of the one-electron molecular ion  $H_2^+$ .

© 2005 Elsevier B.V. All rights reserved.

---

The 1-D electron TDSE in atomic units, *a.u.* ( $e = \hbar = m = 1$ ) is written as

$$i \frac{\partial \psi(x, t)}{\partial x} = \left[ -\frac{1}{2} \frac{\partial^2}{\partial x^2} + V(x) \right] \psi(x, t) = (A + B) \psi(x, t), \quad (2)$$

where  $A = -\frac{1}{2} \frac{\partial^2}{\partial x^2}$ ;  $B = V(x)$ . For time independent potentials, the solution is

$$\begin{aligned} \psi(x, t + \Delta t) &= e^{+\lambda(A+B)} \psi(x, t), \quad \lambda = -i\Delta t, \\ &= S(\lambda) \psi(x, t), \end{aligned} \quad (3)$$

whereas for time-dependent  $V(x, t)$  one must introduce time-ordering operators [3]. A symmetric fourth-order accurate decomposition of  $S = \exp[\lambda(A + B)]$ ,  $S_4$  is obtained as a product of three second-order  $S_2$  (Eq. (1)) operators with time steps  $\gamma\lambda$  and  $(1 - 2\gamma)\lambda$ , [2]

$$S_4^B = e^{\gamma\lambda B/2} e^{\gamma\lambda A} e^{(1-\gamma)\lambda B/2} e^{(1-2\gamma)\lambda A} e^{(1-\gamma)\lambda B/2} e^{\gamma\lambda A} e^{\gamma\lambda B/2}. \quad (4)$$

Permuting  $A$  with  $B$  gives another fourth-order operator  $S_4^A$ . Both involve seven exponential operators with three kinetic energy terms,  $A = T$  in  $S_4^B$  but four such terms in  $S_4^A$ . The accuracy of this decomposition is obtained from

$$\begin{aligned} S - S_4^B &= \frac{\lambda^3}{24} [A + 2B, [A + B]] (2\gamma^3 + (1 - 2\gamma)^3) + \frac{\lambda^4}{24} \\ &\quad \times (3\gamma^3 - 6\gamma^2 + 3\gamma - 1/2) [-2A^2[A, B] \\ &\quad - A[A, B]B \dots] + O(\lambda^5). \end{aligned} \quad (5)$$

Cancellation of corrections of  $O(\lambda^3)$  and  $O(\lambda^4)$  occur simultaneously for real values of  $\gamma = (2 - 2^{1/3})^{-1}$ , thus ensuring fourth-order accuracy. Recently following Suzuki's work [9], Chin has also obtained fourth-order accuracy



We note that  $S_4^B$ , a seven exponential operator, Eq. (5) can be written as

$$S_4^B = e^{j\lambda B/2} e^{j\lambda A} e^{j^* \lambda B/2} e^{(1-2\gamma)\lambda A} e^{j^* \lambda B/2} e^{j\lambda A} e^{j\lambda B/2} + O(\lambda^5),$$

$$\gamma^* = 1 - \gamma, \quad \gamma = (2 - 2^{1/3})^{-1}. \quad (6)$$

Based on this observation we construct a new five exponential third-order operator  $S_3^B$ , (exchanging  $A$  with  $B$  gives  $S_3^A$ )

$$S_3^B = e^{j\lambda B/2} e^{j\lambda A} e^{\lambda B/2} e^{j^* \lambda A} e^{j^* \lambda B/2}, \quad (7)$$

$$S - S_3^B = \frac{\lambda^3}{6} (-3\gamma^2 + 3\gamma - 1) \left( \frac{1}{4} [[A, B], B] - \frac{1}{2} [A, [A, B]] \right) + O(\lambda^4). \quad (8)$$

The  $O(\lambda^3)$  error is cancelled by choosing  $\gamma = \frac{1}{2}(1 \pm i/\sqrt{3})$ .

It is to be noted that the new  $S_3^B$ , Eq. (7) with  $\gamma = a \pm ib$ ,  $a = \frac{1}{2}$ ,  $b = \frac{1}{2\sqrt{3}}$ , can be written equivalently as the product of two  $S_2^B$ 's with complex  $\gamma$ 's,

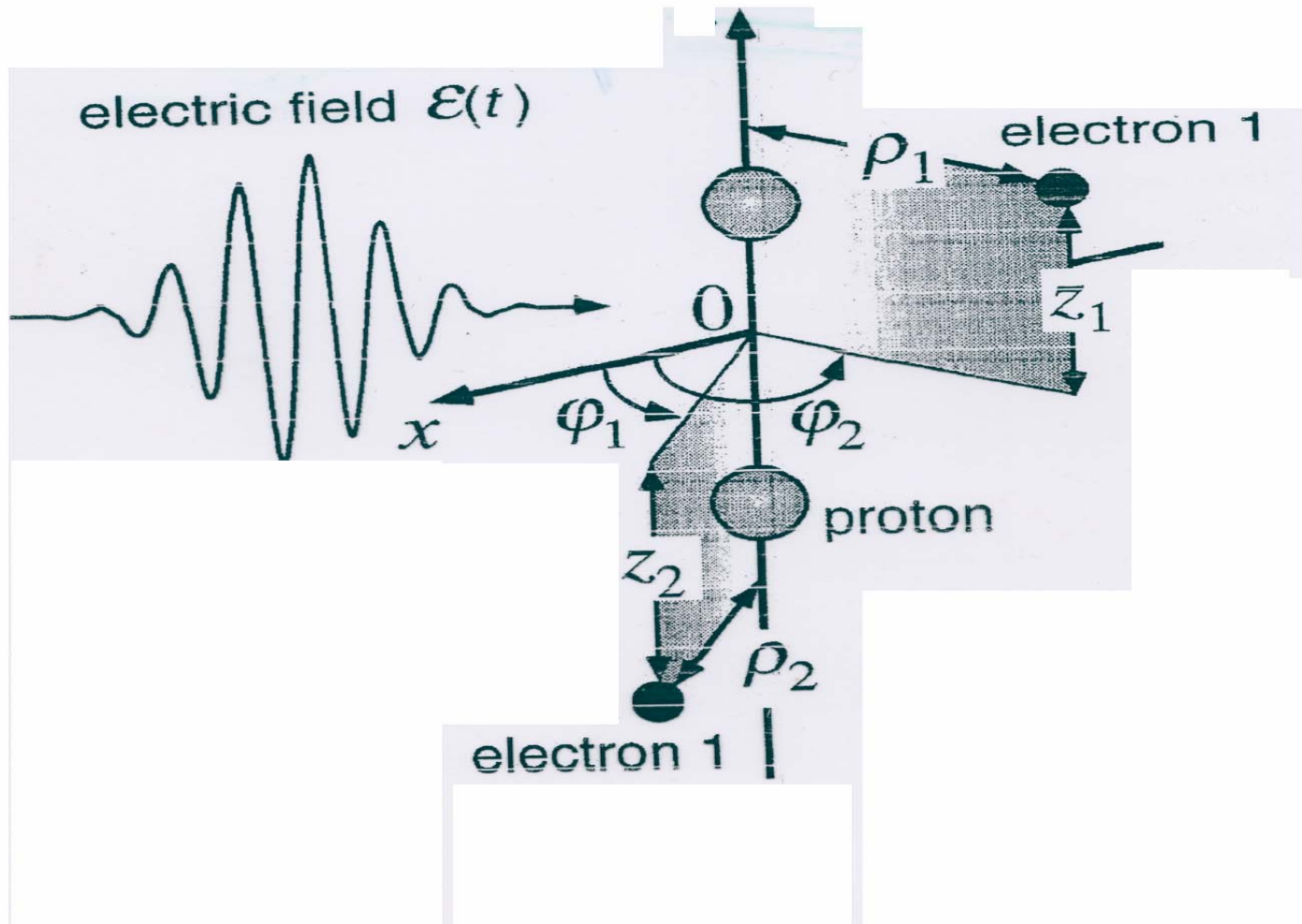
$$S_3^B = (e^{j\lambda B/2} e^{j\lambda A} e^{j\lambda B/2}) (e^{j^* \lambda B/2} e^{j^* \lambda A} e^{j^* \lambda B/2}), \quad (9)$$

$$= S_2^{B'}(\gamma) * S_2^{B'}(\gamma^*) + O(\lambda^4), \quad (10)$$

since  $\gamma + \gamma^* = 1$ .

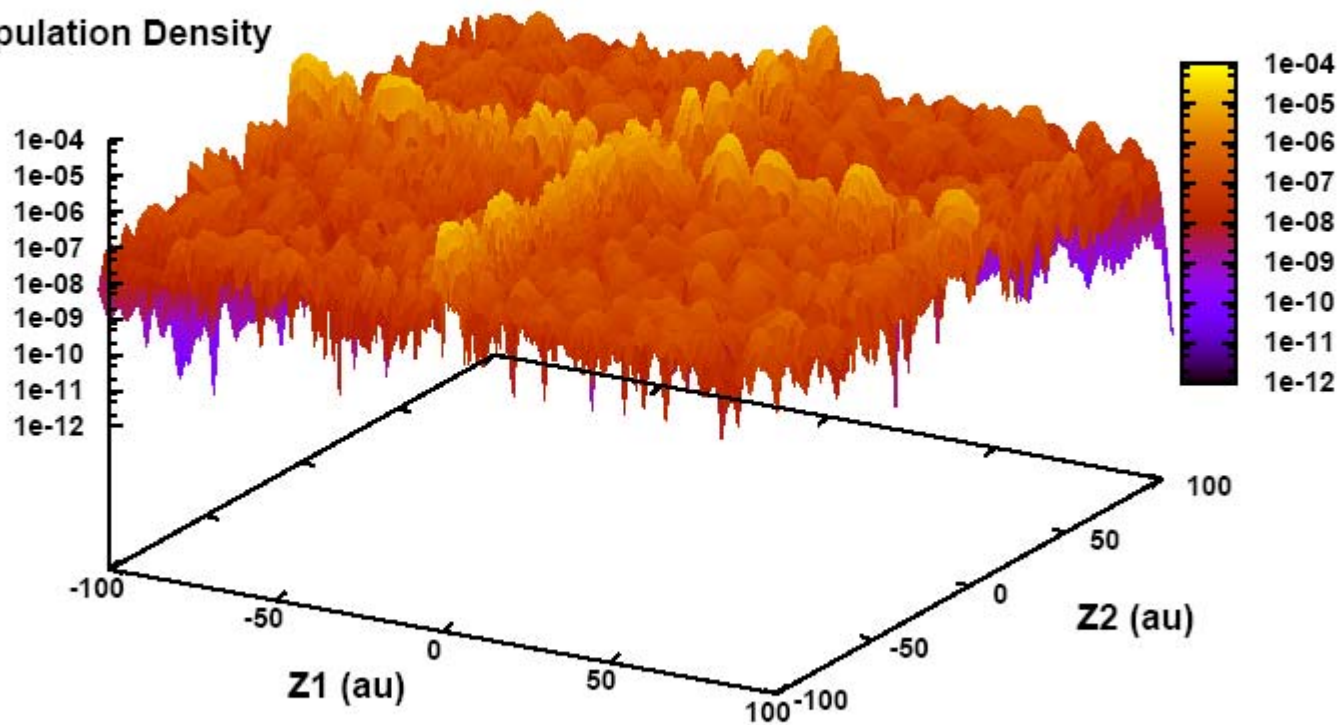
Eqs. (6) and (10) bring out the central role of the second-order operators  $S_2^B = e^{j\lambda B} e^{\lambda A} e^{j^* \lambda B}$ ,  $S_2^A = e^{j\lambda A} e^{\lambda B} e^{j^* \lambda A}$  which are second-order accurate ( $O(\lambda^3)$ ) as in Eq. (1) with  $\gamma = \frac{1}{2}$ . We show next that as suggested by Eqs. (7) and (10), combinations of these  $S_2$ 's with complex  $\gamma = a \pm ib$ , and  $a > 0$ , gives new high-order evolution operators.

$$N_p = \underbrace{10^3}_{z_1} \times \underbrace{10^3}_{z_2} \times \underbrace{10^2}_{\hat{c}_1} \times \underbrace{10^2}_{\hat{c}_2} \times \underbrace{10^2}_{\phi} \simeq 10^{12} \times \underbrace{10^2}_p \simeq 10^{14}$$



$\text{H}_2 (\text{X}^1\Sigma_g^+)$ :  $I=3\times 10^{15}\text{W}/\text{cm}^2$ ,  $\lambda=800\text{nm}$ ,  $T = 6$  cycles

Population Density



## NEWS

# The petaflop challenge

IBM's announcement on 28 June that it was about to smash the petaflop speed barrier could herald a new era in computing. But unless the research and computing communities get their programming act together, they risk having few scientific applications that can take advantage of this huge increase in power, say experts.

Called Blue Gene/P, the first of the new high-powered computers should be operational next year, and IBM has already lined up potential customers in the United States, Germany and Britain. The largest planned configuration for the machines would run continuously at 1,000 trillion floating-point operations per second, or teraflops, and be capable of peak speeds of up to 3,000 teraflops (3 petaflops). That would make it between three and ten times faster than the machine that tops the latest TOP500 list of supercomputers, the IBM Blue Gene/L at Lawrence Livermore National Laboratory in California, which peaks at 960 teraflops.

"I never yearned," says Ray Bair, head of the Argonne Leadership Computing Facility at the Argonne National Laboratory in Illinois, which has worked with IBM on developing the Blue Gene/P and which will host a version of the hardware. "We're crossing a threshold." Bair adds, claiming that the increased power will let allow researchers to build and run models in the way they have always wanted.

At a price of around \$100 a gigaflop, petaflop computers will start off in the \$100-million range. A great deal of the added speed that money will buy simply comes from more processors. Supercomputer designers began taking parallel processing seriously in the 1990s, but few machines have been designed to work with more than 10,000 processors. In 2005, Blue Gene/L, which is almost three times as fast in its nearest competition, marked a significant step up with 151,372 processors. A 3-petaflop Blue Gene/P will be an 884,736 — a multitude that brings with it problems as well as promise.

The rapid recent growth in supercomputing power — Blue Gene/L is as powerful as the whole of 2002's TOP500 list combined — has come mostly from increases in the performance of the computer's component processors. But a few years ago the process came to a grinding halt, says Ken Szebeni, head of Blue Gene applications at IBM's Thomas J. Watson Research Center in Yorktown Heights, New York. As the processors got faster and denser, they began suffering from disproportionate increases

in power consumption and heat output.

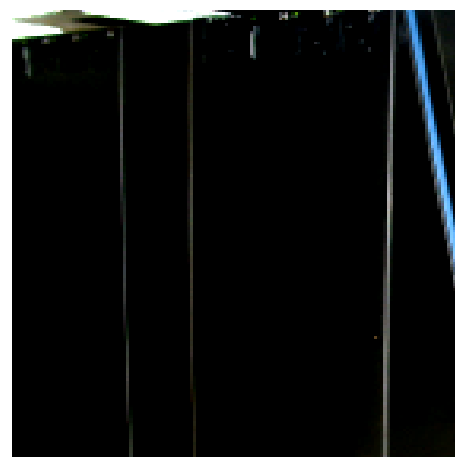
To combat this, chipmakers made a historic switch. Since 2004, they have concentrated on increasing the number of processors on a chip, allowing the speed at which individual processors operate to plateau. So the dual- and quad-chip now common in laptops, offering two or four processors, may well be upgraded to 128 or 256 cores by 2015. This means that the cheap Linux supercomputing clusters common in universities would have hundreds of thousands of processors, and dedicated supercomputers might have hundreds of millions. The processors will not necessarily be blazingly fast — Blue Gene/P's 600-MHz chips are little faster than a Pentium III from 1998. But with their numerical advantage they won't have to be.

This new reliance on parallel processing for increased performance means that companies from Microsoft to Nintendo will have to rethink their software — and so will scientists. A few scientific applications fall into the freewheel category called embarrassingly parallel problems: Genome analysis using BLAST software to compare sequences and mass spectrometry for proteomics are generally fairly easy to parallelize, says Leroy Hood, president of the Institute for Systems Biology in Seattle, Washington. Each processor can take on a specific task without much reference to what all the others are doing. But other sorts of problems, in which many of the calculations depend on other calculations being done elsewhere, are not so tractable.

For the moderate levels of parallelism seen to date, it is possible to get by with the current practice of writing code, and designing models, in terms of linear sequences of instructions and then parallelizing once satisfied. To get the most out of massive parallel clusters and machines, that will no longer be an option. "Coding models remains tedious as many as a million processors is a new challenge we have to meet," says Tim Palmer of the European

**"The scientific community is not very good at software development."**

Centre for Medium-Range Weather Forecasts in Reading, UK, who is interested in petaflop machines for climate modelling. "We have no choice but to follow the hardware trends."

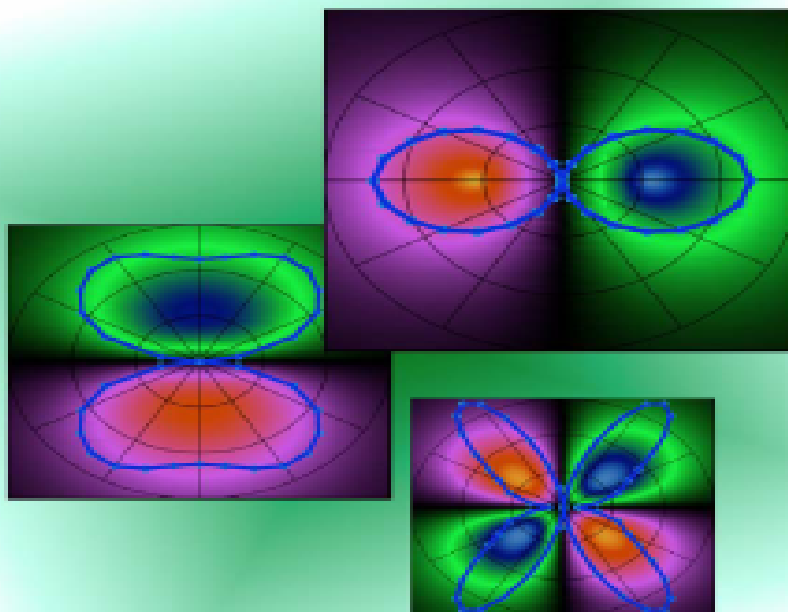


Centre for Medium-Range Weather Forecasts in Reading, UK, who is interested in petaflop machines for climate modelling. "We have no choice but to follow the hardware trends."

Scientists need to shift to thinking in parallel from the outset, designing hypotheses and code accordingly, says Horst Simon, associate lab director for computing at Lawrence Berkeley National Laboratory, California. He describes what is needed as nothing short of a "revolution in scientific programming". Such a revolution has been brewing for decades, but there hasn't been much awareness of the barrier. "The high-performance computing community has been working on the parallel-programming problem for over 25 years. And frankly, we don't have much to show for it," wrote Intel researcher Timothy Mattson on his company's research blog last week. "On the software front, it's chaos."



Rapport annuel 2008  
1<sup>er</sup> janvier au 31 décembre



## NEW TECHNIQUE: LIED LASER INDUCED ELECTRON DIFFRACTION

T.Zuo, A.D. Bandrauk, and P.B. Corkum,  
Chem. Phys. Lett. , 313 (1996).

$H_2^+$  in a  $\delta$ - pulse (attosecond)

**1as=10<sup>-18</sup>**

$$E(t) = F\delta(t)$$

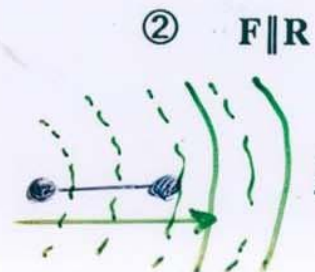
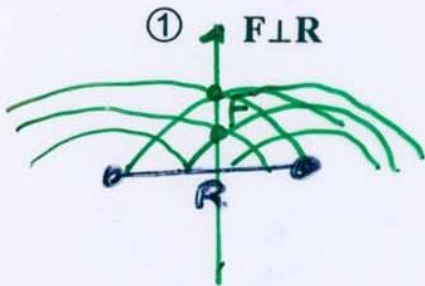
$$\varphi(\vec{p}) = \phi_{1\sigma_g}(\vec{p} + \vec{F})$$

$$= 2 \cos \left[ (\vec{p} + \vec{F}) \cdot \frac{\vec{R}}{2} \right] \phi_{1s}(\vec{p} + \vec{F})$$

$$\varphi(p) = 2 \cos \left( \frac{\vec{p} \cdot \vec{R}}{2} \right) \phi_{1s}(\vec{F} + \vec{p})$$

**max** at  $p = \frac{2m\pi}{R \cos \theta}$

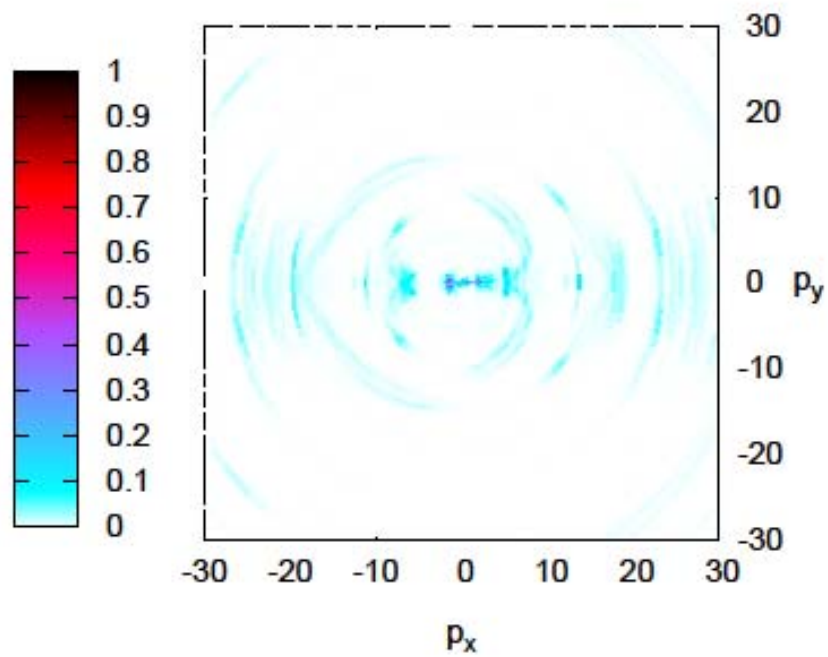
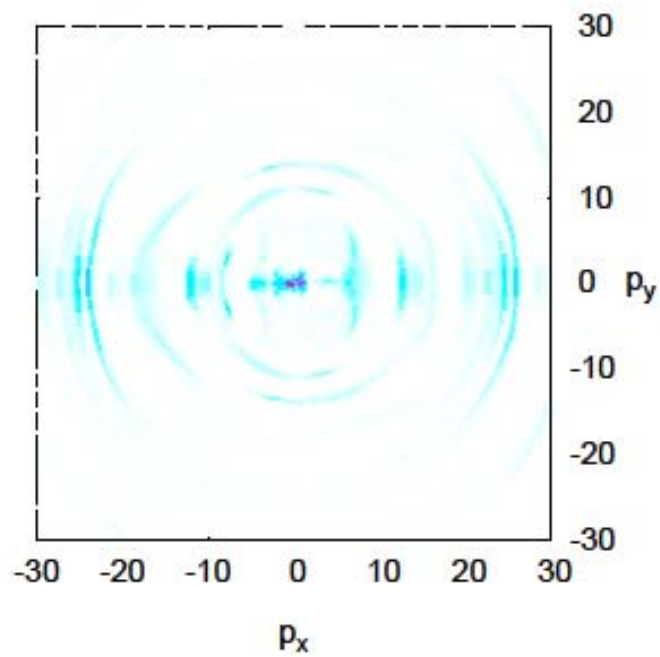
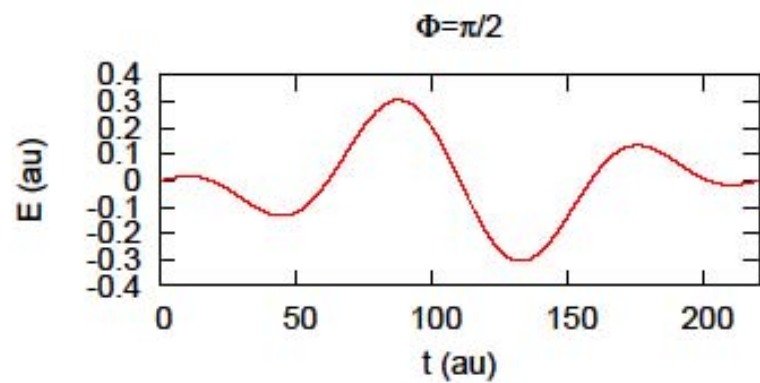
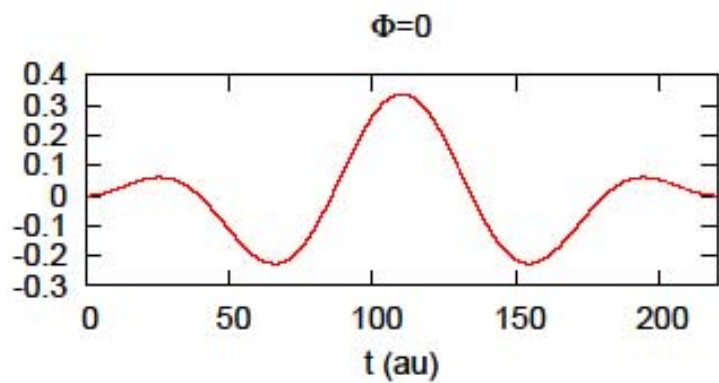
**min** at  $p = \frac{(2m+1)\pi}{R \cos \theta}$

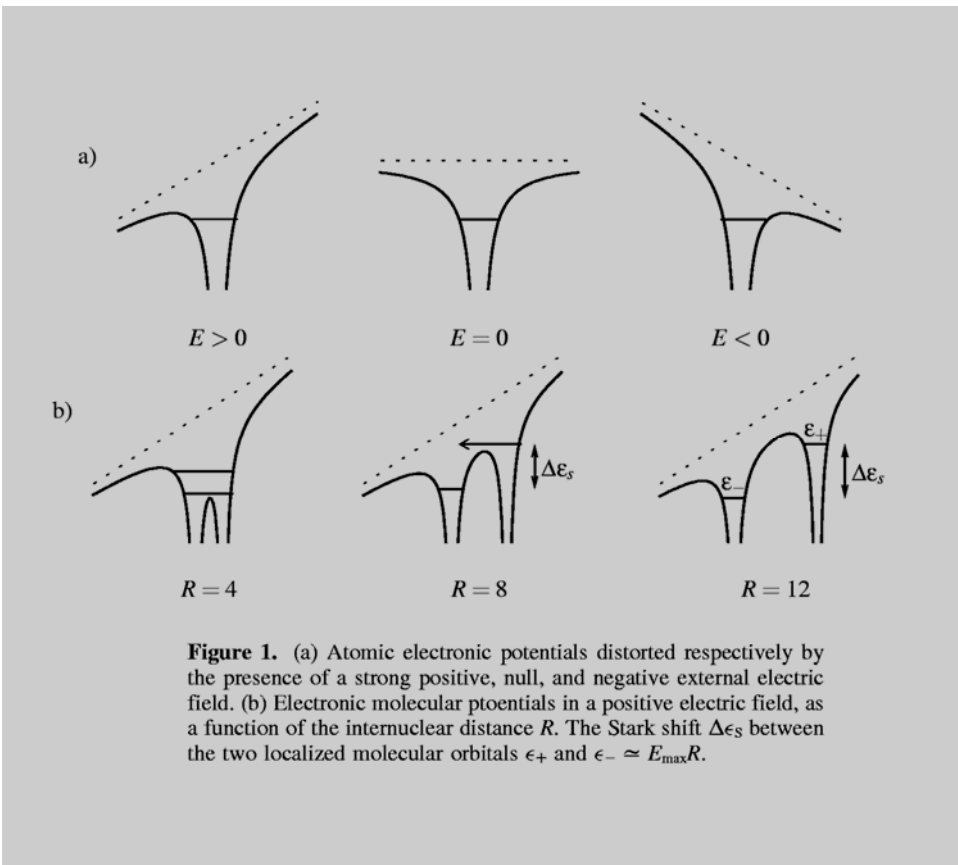


$$\varphi(p) = 2 \cos \left[ \frac{FR}{2} \left( 1 + \frac{p \cos \theta}{F} \right) \right] \phi_{1s}(\vec{F} + \vec{p})$$

**Small p:**  $\begin{cases} \text{max} \\ \text{min} \end{cases} FR = \begin{cases} 2m\pi \\ (2m+1)\pi \end{cases}$

**large p:**  $(FR + pR \cos \theta) \rightarrow \frac{2m\pi}{(2m+1)\pi}$





P. B. Corkum, PRL,  
71, 1994 (1993).

T. Zuo and A. D. Bandrauk,  
PRA, 52, R2511 (1995).



# Nuclear fusion from explosions of femtosecond laser-heated deuterium clusters

T. Ditmire, J. Zweiback, V. P. Yanovsky, T. E. Cowan, G. Hays & K. B. Wharton

Laser Program, L-477, Lawrence Livermore National Laboratory, Livermore, California 94550, USA

As a form of matter intermediate between molecules and bulk solids, atomic clusters have been much studied<sup>1</sup>. Light-induced processes in clusters can lead to photo-fragmentation<sup>2,3</sup> and Coulombic fission<sup>4</sup>, producing atom and ion fragments with a few electronvolts (eV) of energy. However, recent studies of the photoionization of atomic

cluster) are ionized, electrons undergo rapid collisional heating for the short time ( $< 1$  ps) before the cluster disassembles in the laser field<sup>19</sup>. Through various collective and nonlinear processes, the laser rapidly heats the electrons to a non-equilibrium state (with mean

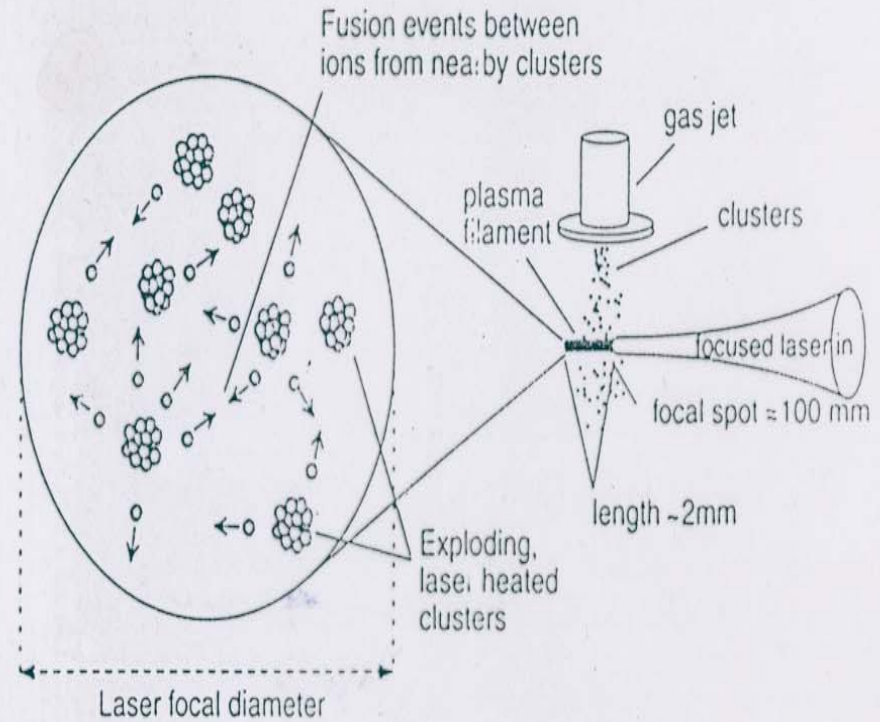
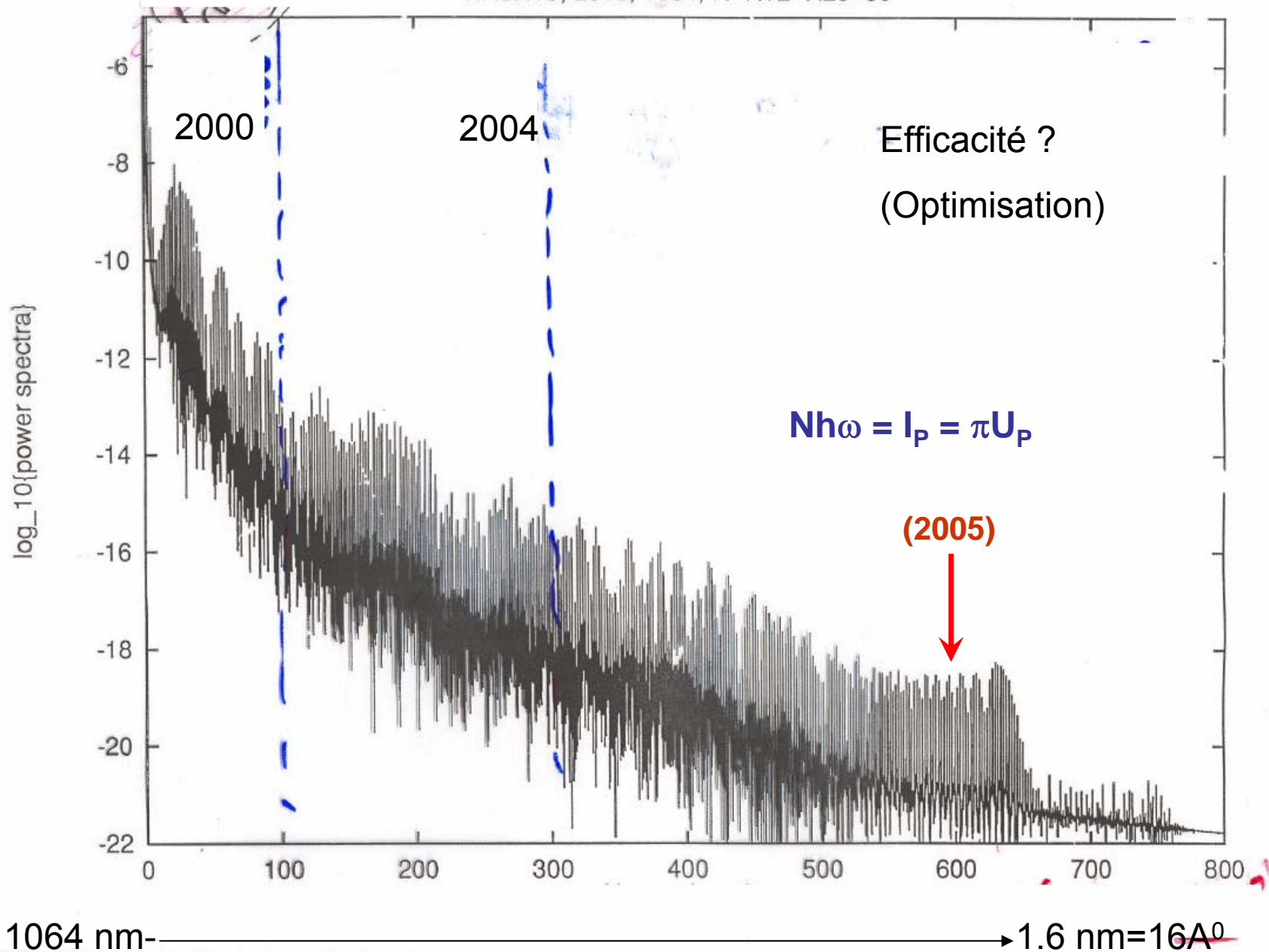


Figure 1 Layout of the deuterium cluster fusion experiment.



Step 1: get spectrum

$$a(t) = \langle \psi(t) | \dot{z} | \psi(t) \rangle$$

$$a(\omega) = \frac{1}{2\pi} \int_{-\infty}^{+\infty} a(t) e^{-i\omega t} dt$$

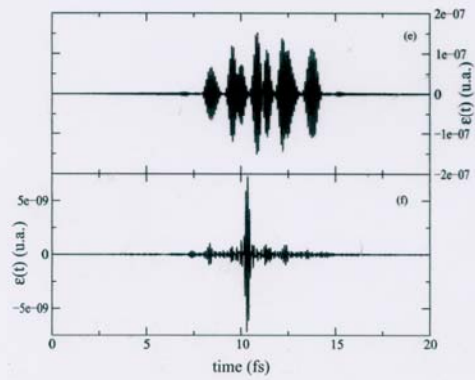
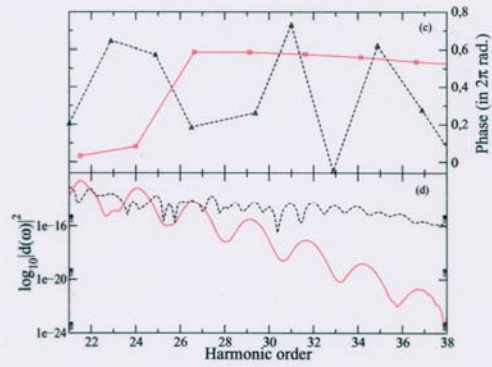
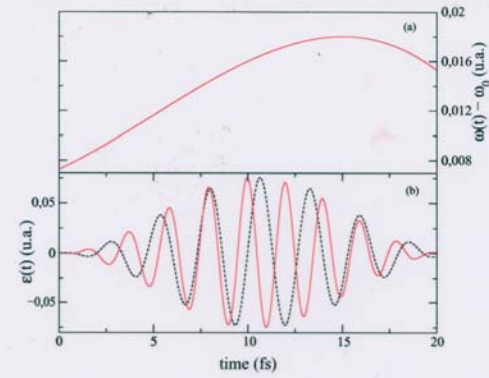
Step 2: select frequency region between  $\omega_1 < \omega < \omega_2$

Step 3: come back to time domain

$$\tilde{a}(t) = \int_{\omega_1}^{\omega_2} a(\omega) e^{i\omega t} d\omega$$

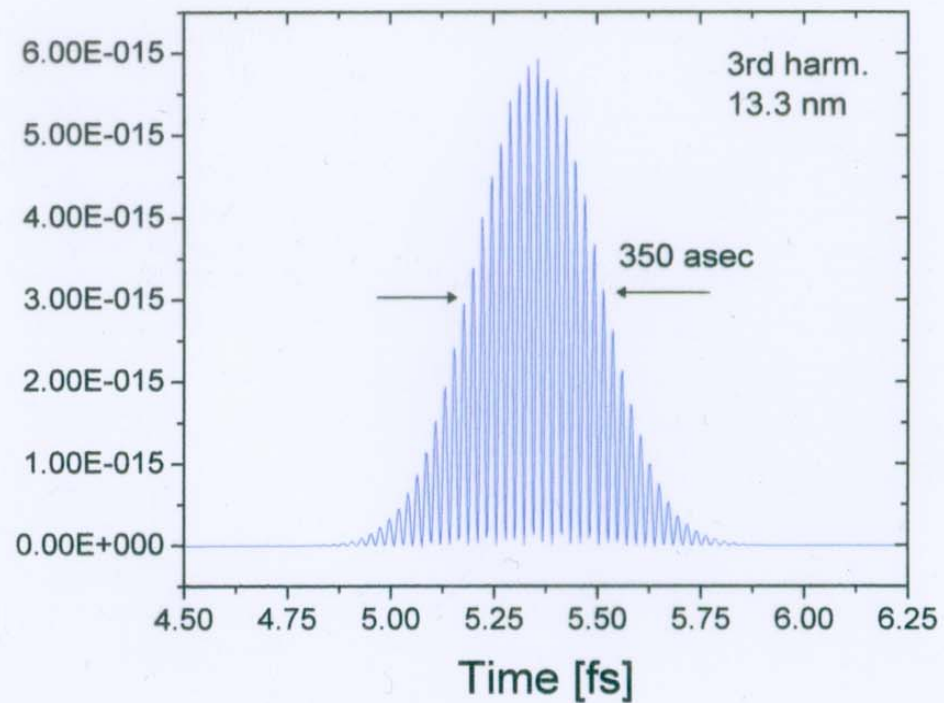
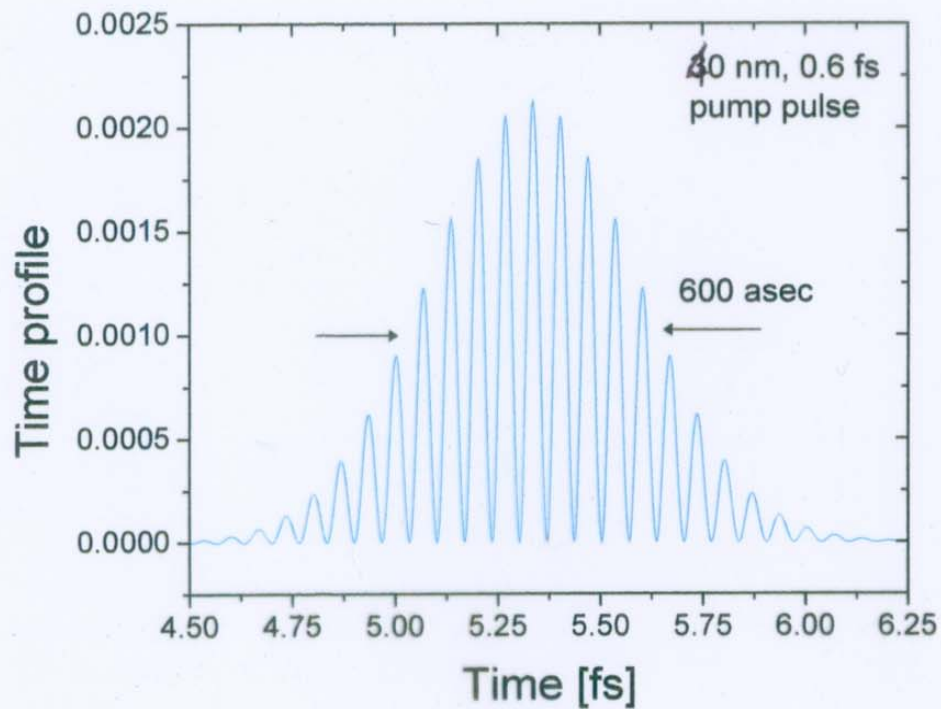
$$\Delta \omega = \omega_2 - \omega_1$$

$$\tau \approx \frac{1}{\Delta \omega} \rightarrow \text{attosecond} = 3 \text{ Angstroms} (10^{-8} \text{ cm}) / c (3 \times 10^{10} \text{ cm/s})$$



Yedder, LeBris, Chelkowski, Bandrauk, PRA 69, 041802 (2004)

# Frequency-up conversion, 1st -->3rd harmonics



LQ11676

**Effect of Nuclear Motion on Molecular High-order Harmonics  
and on Generation of Attosecond Pulses in Intense Laser Pulses**

André D. Bandrauk, Szczepan Chelkowski, Shinnosuke Kawai, and Huizhong Lu

*Département de Chimie, Université de Sherbrooke, Sherbrooke, Qc, J1K 2R1 Canada*

**Abstract**

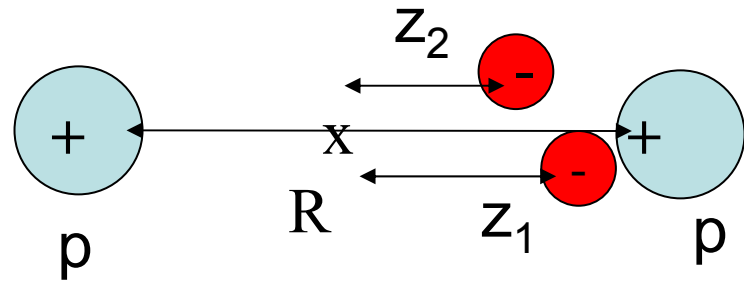
We calculate harmonic spectra and shapes of attosecond pulse trains using numerical solutions of Non-Born Oppenheimer time-dependent Schrödinger equation for 1-D  $H_2$  molecules in an intense laser pulse. A very strong signature of nuclear motion is seen in the time profiles of high order harmonics. In general the nuclear motion shortens the part of the attosecond pulse train originating from the first electron contribution but it may enhance the second electron contribution for longer pulses. The shape of time profiles of harmonics can thus be used for monitoring the nuclear motion.

PACS numbers: 42.65.Ky, 42.65.Re, 42.50.Hz, 32.80.Rm

Phys Rev Lett( 2008,)101,153901

J Phys B –to appear 2009

La dynamique de 4-particules:  
 $p+p+e^-+e^-$  décrite par l'éq. de  
 Schrödinger solutionnée numé-  
 riquement



Équation de Schrödinger dépendant de temps pour une molécule  $H_2$

exposée au champ laser intense décrit par :  $E(t) = \epsilon(t) \cos(\omega_L t)$

(polarisation linéaire)

a.u.  $e = \hbar = m_e = 1$ )

$$i \frac{\partial \psi(z_1, z_2, R, t)}{\partial t} = [H_e + H_N + V(z_1, z_2, t)] \psi(z_1, z_2, R, t), \quad (1)$$

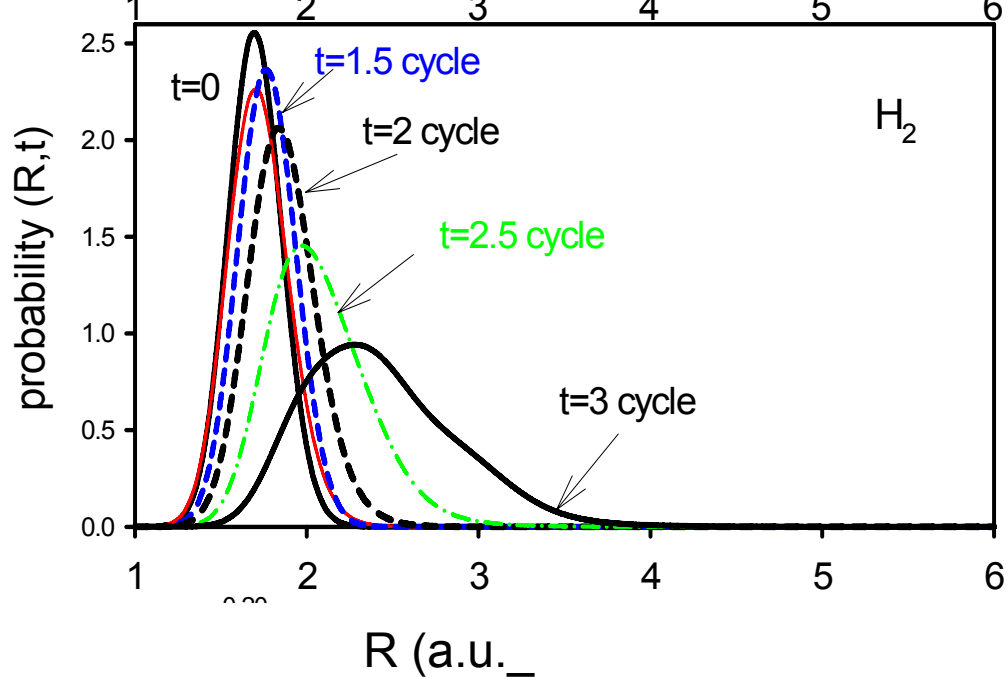
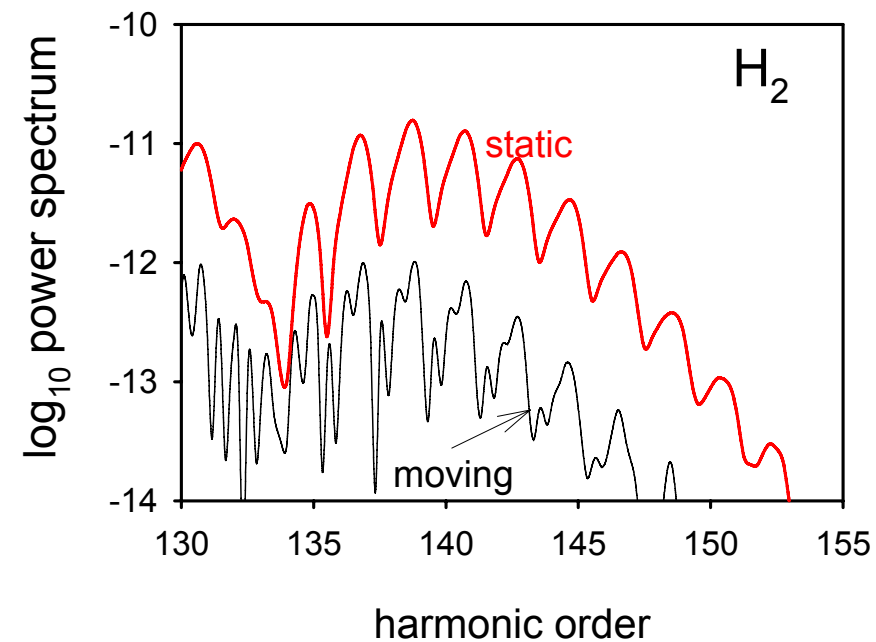
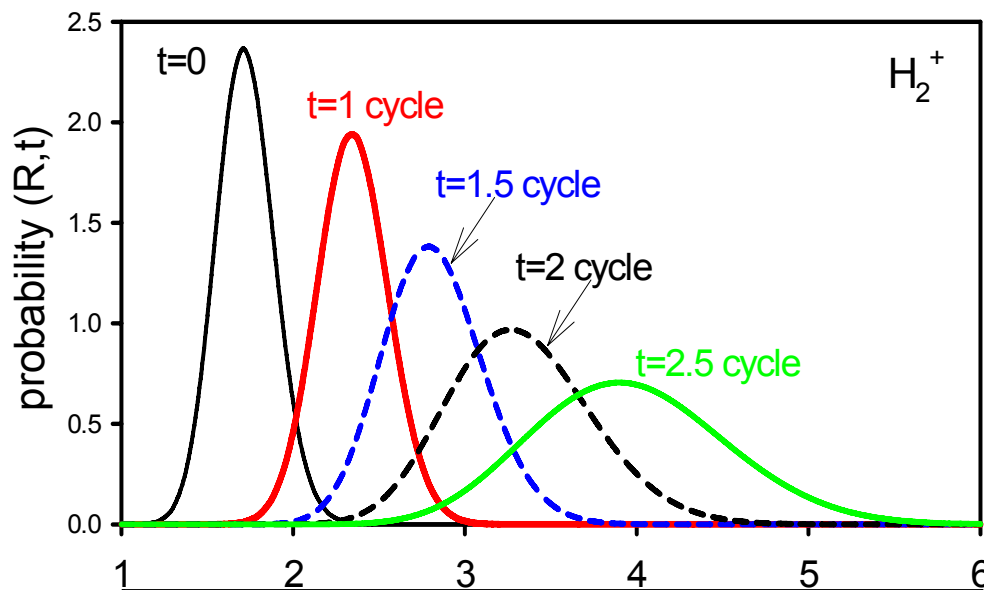
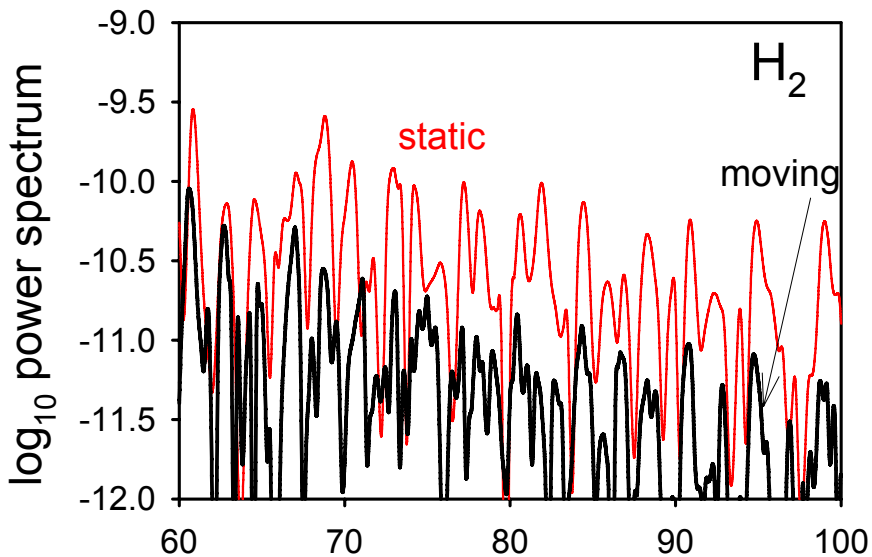
$$H_e = \sum_{i=1}^2 \left[ -\frac{1}{2} \frac{\partial^2}{\partial z_i^2} - \frac{1}{[(z_i + R/2)^2 + c]^{1/2}} - \frac{1}{[(z_i - R/2)^2 + c]^{1/2}} \right] + V_{rep}(z_1, z_2) \quad (2)$$

$$V_{rep}(z_1, z_2) = \frac{1}{[(z_1 - z_2)^2 + d]^{1/2}}, \quad ; H_N = -\frac{1}{2M} \frac{\partial^2}{\partial R^2} + \frac{1}{R} \quad (3)$$

$$V(z_1, z_2, t) = (z_1 + z_2) \epsilon(t) \cos(\omega_L t) \quad (4)$$

$$d(t) = \langle z_1 + z_2 \rangle = \int_{-\infty}^{\infty} dz_1 \int_{-\infty}^{\infty} dz_2 \int_0^{\infty} dR \psi^*(t)(z_1 + z_2) \psi(t)$$

1 cycle=110.32 a.u.



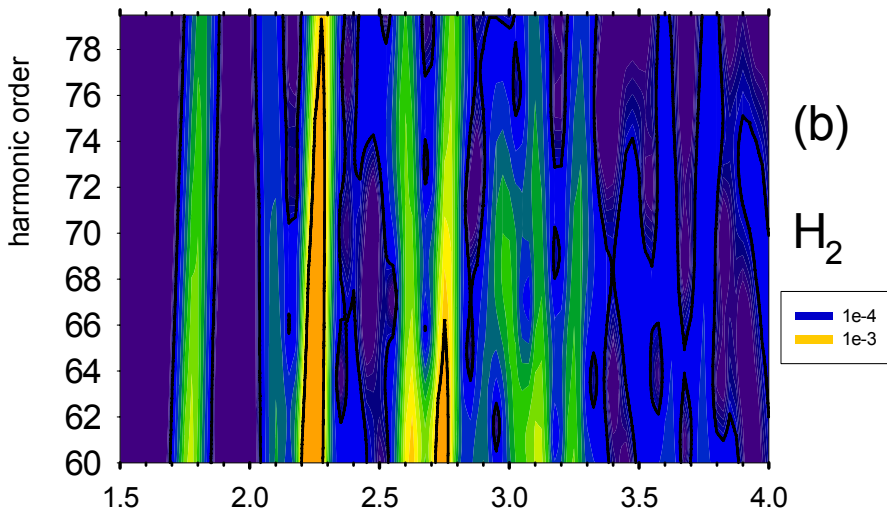
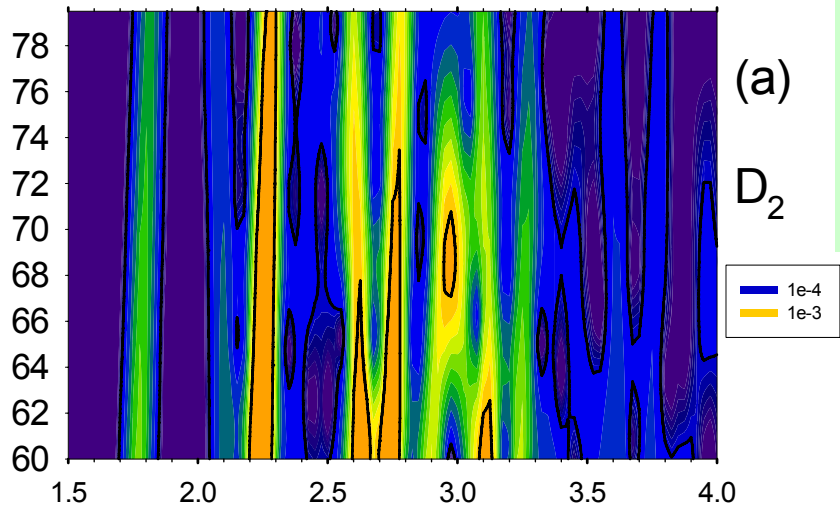


Analyse en temps-frequence  
de Gabor (ondelettes):

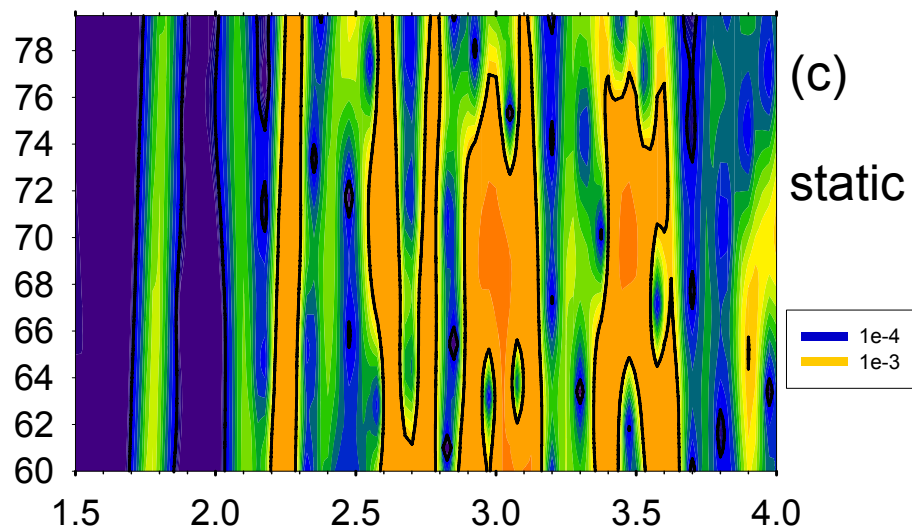
$$= d_G(t, \omega) = \int_{-\infty}^{\infty} dt' G(t, t') \exp(-i\omega t) d(t)$$

$$G(t-t') = \exp\left[-\frac{(t-t')^2}{2\sigma_0^2}\right], \quad \sigma_0 = 0.1 \text{ fs}$$

$$d_G(t, \omega) = \text{cte} \int_{-\infty}^{\infty} d\omega' e^{-b(\omega-\omega')^2} e^{i\omega't} d_F(\omega')$$



$|d_G(t, \omega)|$  - profile temporaire des  
impulsions atto dans un train,  $\Delta\omega \sim 5-10 \omega_L$



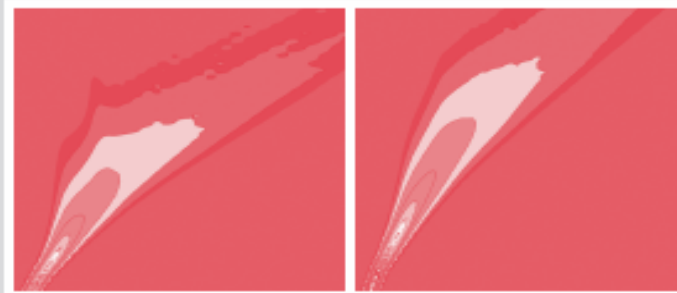
temps (periodes du laser  $T_{\text{las}}$ ) ,  $T_{\text{las}} = 2.67 \text{ fs}$

# Journal of Physics B

Atomic, Molecular  
and Optical Physics

Volume 42 Number 7 14 April 2009

**Incorporating Journal of Optics B: Quantum and Semiclassical Optics**



[www.iop.org/journals/jphysb](http://www.iop.org/journals/jphysb)

**IOP** Publishing

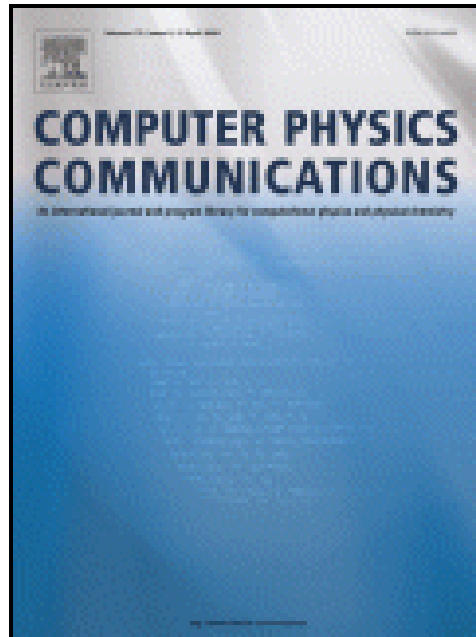
# Top 25 Hottest Articles

## ScienceDirect Top 25 Articles Overall

**October - December 2007**



RSS



### **A numerical Maxwell–Schrödinger model for intense laser–matter interaction and propagation**

E. Lorin<sup>a, b, \*</sup>, S. Chelkowski<sup>c</sup> and A. Bandrauk<sup>d</sup>

<sup>a</sup>Centre de Recherche en Mathématiques de Montréal, University of Montréal, Canada

<sup>b</sup>University of Ontario, Institute of Technology, Oshawa, Canada

<sup>c</sup>Université de Sherbrooke, laboratoire de chimie théorique, Canada

<sup>d</sup>Université de Sherbrooke, laboratoire de chimie théorique, Centre de Recherche en Mathématiques de Montréal, Canada Research Chair, Canada

# Model

Coupling of macroscopic Maxwell's equations with many TDSE's.

Lorin, Chelkowski, Bandrauk, *Comput. Phys. Comm.* vol. 177 (2007)

$$\left\{ \begin{array}{l} \partial_t \mathbf{B}(\mathbf{r}, t) \\ \partial_t \mathbf{E}(\mathbf{r}, t) \\ \nabla \cdot \mathbf{B}(\mathbf{r}, t) \\ \nabla \cdot (\mathbf{E}(\mathbf{r}, t) + \mathbf{P}(\mathbf{r}, t)) \\ \\ \mathbf{P}(\mathbf{r}, t) = n(\mathbf{r}) \sum_{i=1}^m \mathbf{P}_i(\mathbf{r}, t) \\ i \partial_t \psi_i(\mathbf{r}', t) \end{array} \right. = \begin{array}{l} -\nabla \times \mathbf{E}(\mathbf{r}, t) \\ \nabla \times \mathbf{B}(\mathbf{r}, t) - 4\pi \partial_t \mathbf{P}(\mathbf{r}, t) \\ 0 \\ 0 \\ \\ n(\mathbf{r}) \sum_{i=1}^m \chi_{\Omega_i}(\mathbf{r}) \int_{\mathbb{R}^3} \psi_i \mathbf{r}' \psi_i^* \\ -\frac{\Delta_{\mathbf{r}'}}{2} \psi_i + \mathbf{r}' \cdot \mathbf{E}_{\mathbf{r}_i} \psi_i + V_c \psi_i, \\ \forall i \in \{1, \dots, m\} \end{array}$$

The numerical model is the one presented in [19], where the gas domain is divided in small cells of gas denoted by  $\Delta v$  (corresponding the  $\Omega_i$ 's of Section 2) and in which we solve 1 TDSE, representing the  $n\Delta v$  molecules of the cell. In practice 3d Maxwell's equations are solved in parallel with  $\sim 140,000$  1d TDSE's, see Fig. 5 and [17]. We then represent at

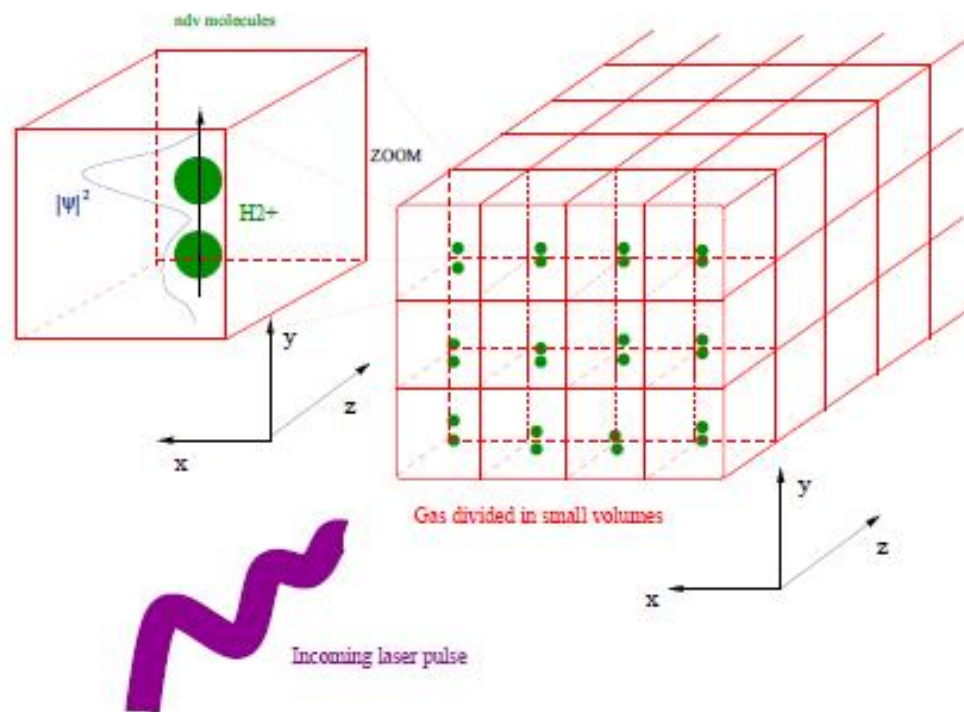


Figure 5: Numerical geometry

# Beyond the paraxial & SVEA approximation

Under the paraxial and SVEA approximation equation on

$\mathbf{E}(x, y, z, t) = \mathcal{E}(x, y, z, t)e^{i(kz - \omega t)}\mathbf{e}_y$  with  $\mathcal{E}$  the envelope [Bergé et al.](#)

[Physica D, 176 \(2003\)](#), [Couairon, Mysyrovicz, Phys. Report 441 \(2007\)](#):

$$\partial_z \mathcal{E} = \frac{i}{2k} \Delta_{\perp} \mathcal{E} + ik_0 n_2 |\mathcal{E}|^2 \mathcal{E} - \frac{ik_0}{2n_0 \rho_c} \rho \mathcal{E}, \quad \partial_t \rho = \sigma_K |\mathcal{E}|^{2K} \rho_{\text{atm}}$$

- $K$  the number of photons in multi-photon ionization,  $K = \langle U_i / \hbar\omega_0 + 1 \rangle$  ( $U_i$  ionization potential of the medium)
- $\sigma_K$  the coefficient of the multi-photon ionization rate
- $\rho_{\text{atm}}$  the neutral atom density

Focusing and defocusing effects clearly identified numerically and theoretically for long pulses ([Bergé, Couairon, Ginibre, Fibich, Sulem, etc](#))

# Numerical data

## Numerical data

- $\sim 140,000$  1D TDSE's solved in parallel
- 3D Maxwell's equations
- $\sim 30h$  on 128 processors of `mammoth` (RQCHP) [Lorin, Bandrauk, IEEE proceed. \(2008\)](#) We represent at time different times  $t_k$  the transversal cut of the pulse at  $z_k$  such that  $|E_y(0, 0, z, t_k)|$  is maximal at  $z_k$  on  $(Oz)$ . In other words

We represent transversal cuts of the beam

- At  $t_k$  fixed, we denote  $|E_y|_\infty = \max_z |E_y(0, 0, z, t_k)|$  the maximal value on the  $(Oz)$  axis reached in  $z_k$
- We draw  $E_y(x, 0, z_k, t_k) / |E_y|_\infty$  in order to have normalized graphs to compare with vacuum

Results I -  $I \sim 2 \times 10^{16} \text{W}\cdot\text{cm}^{-2}$ ,  $n_0 \sim 3 \times 10^{20} \text{mol}\cdot\text{cm}^{-3}$

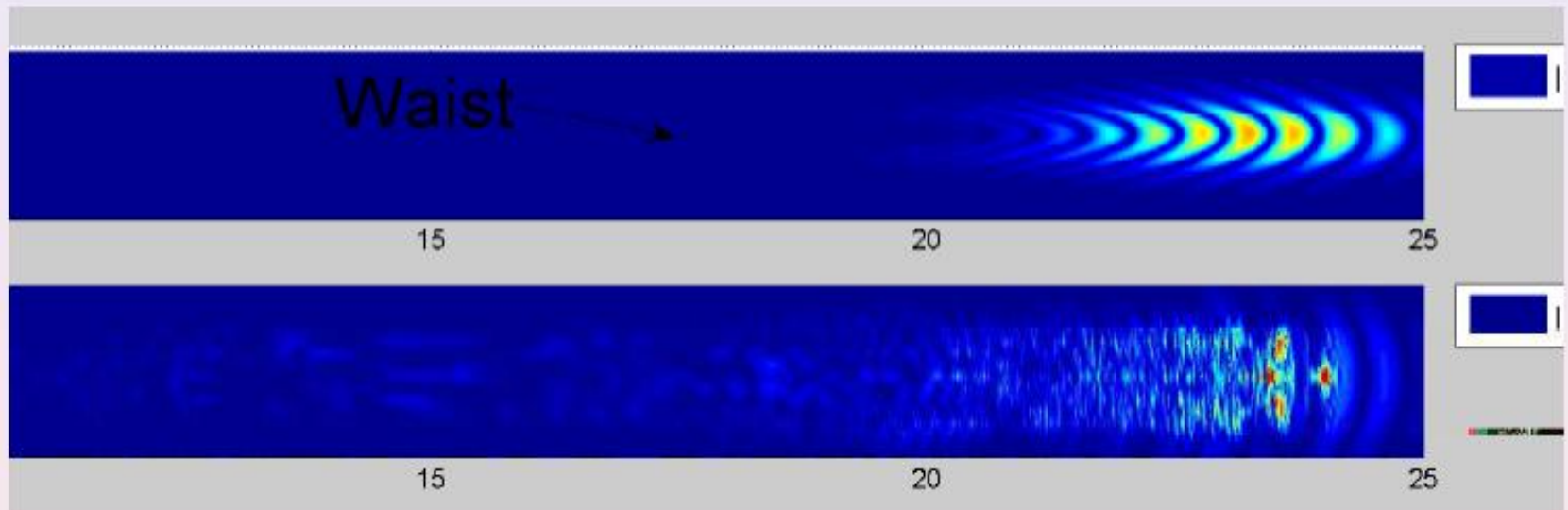


Figure:  $|E_y|^2$  -  $4.5\mu\text{m}$  after the waist in vacuum and gas



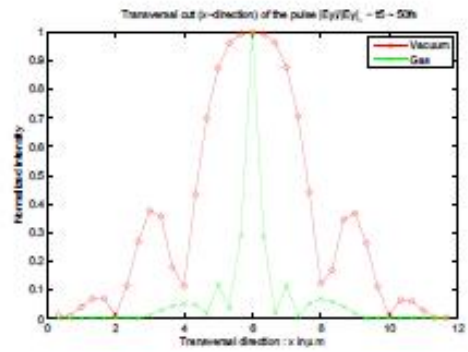


Figure 11: Pulse thickness during propagation  $7\mu m$  after the waist

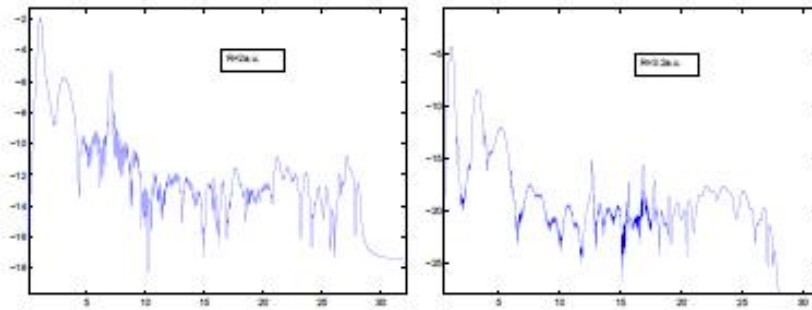


Figure 12: Electric field harmonics  $R = 2.a.u.$ ,  $R = 3.2a.u.$

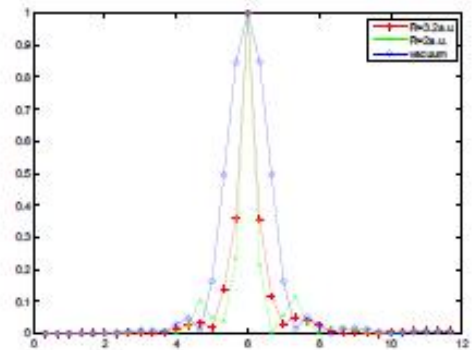


Figure 13: Electric field transversal cut  $R = 2.a.u.$ ,  $R = 3.2a.u.$

# Improvement of the model I - microscopic approach

Another approach is presented in [Lorin, Bandrauk, Chelkowski, Num. Methods for Partial Diff. Eq., \(2008\)](#). A method to transmit free electron from a molecule to another. Based on a particular choice of boundary conditions (Volkov)

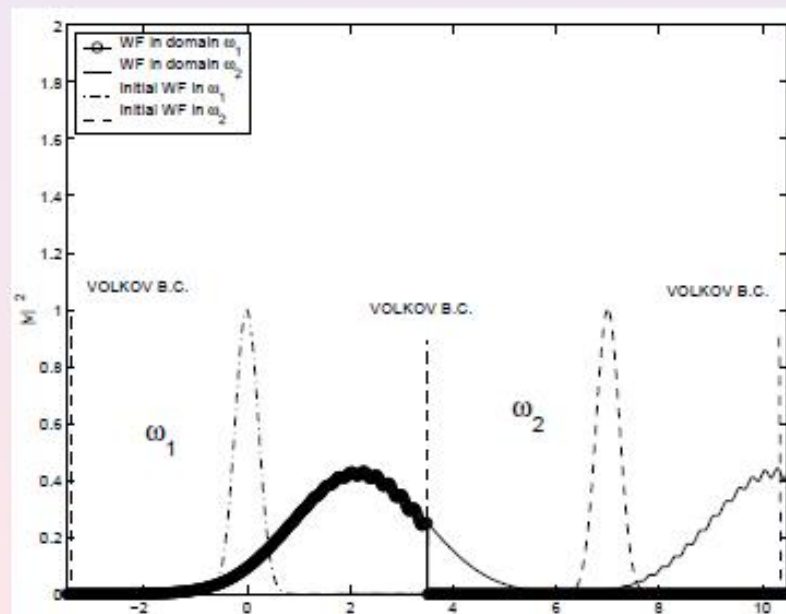
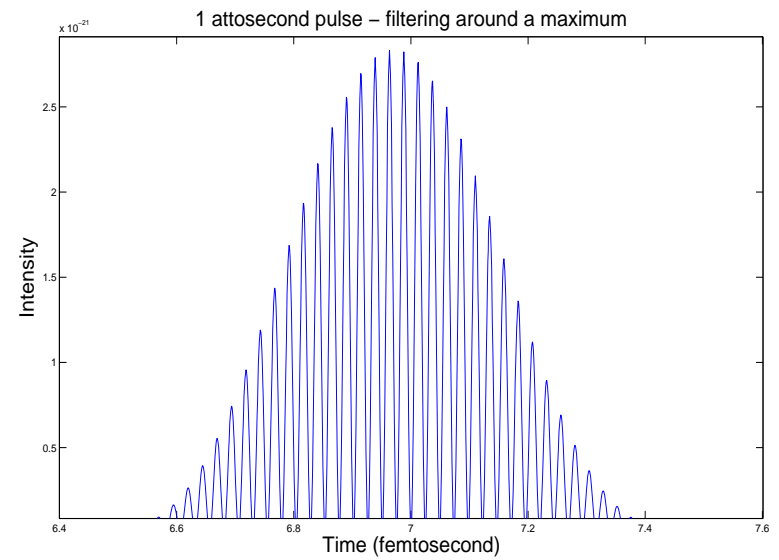
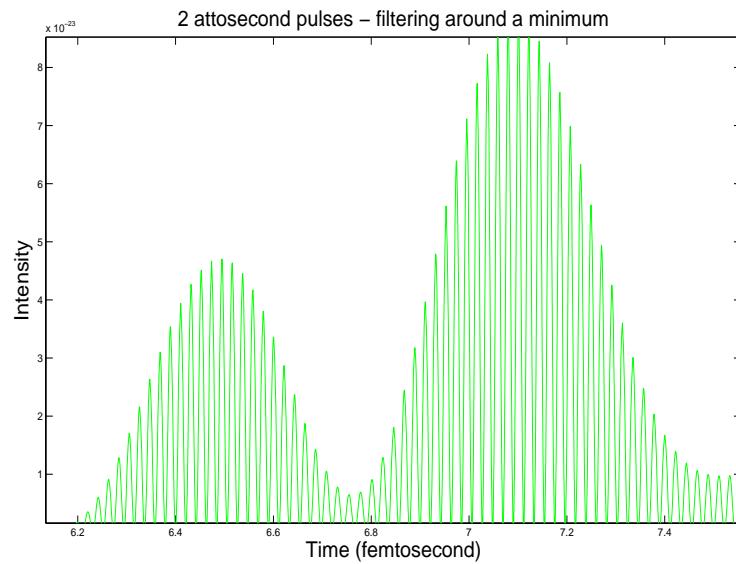
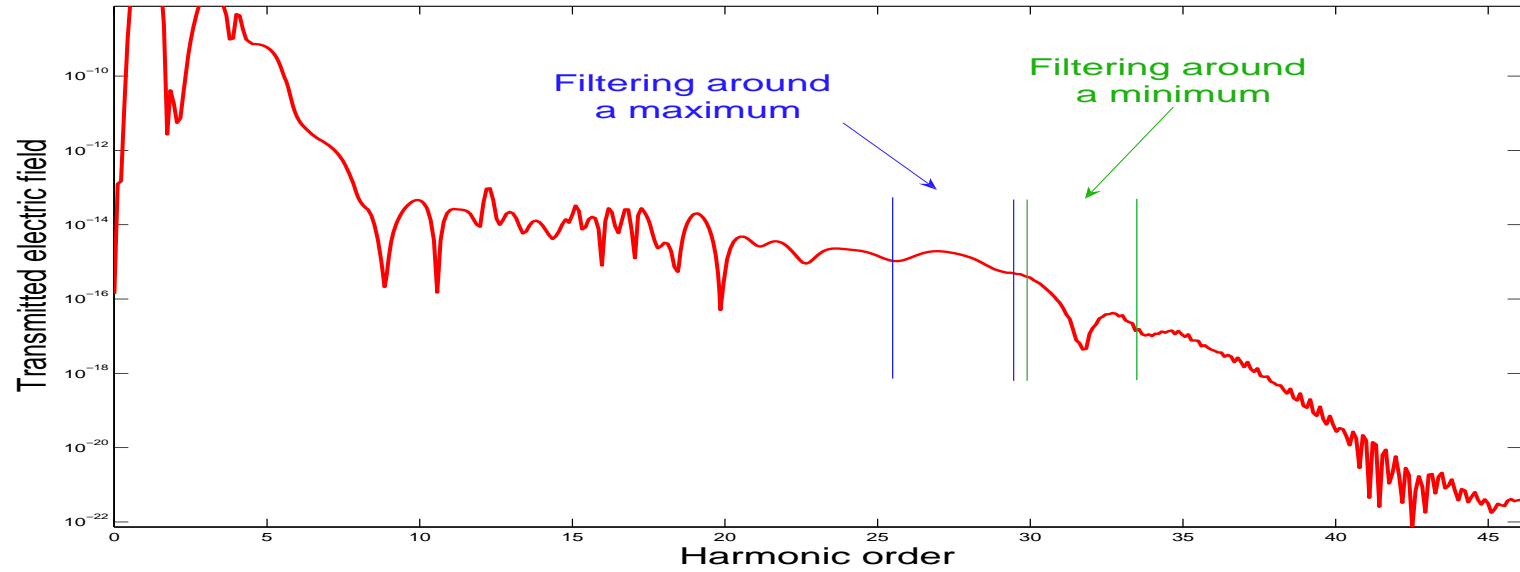
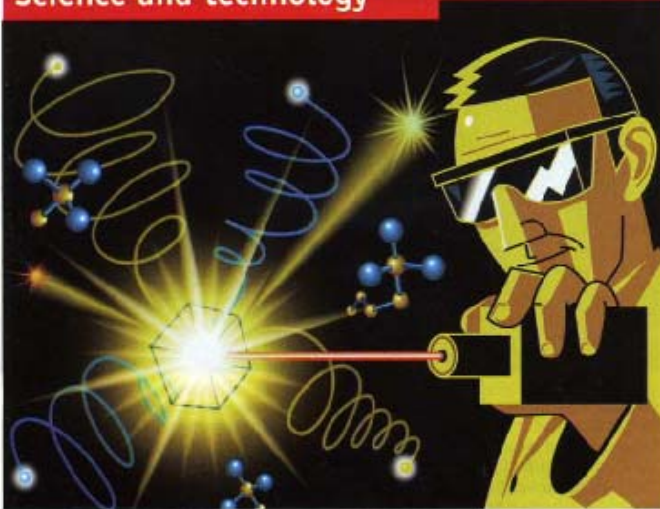


Figure: Free electron transmission

Transmitted electric field harmonic – Short propagation



Two (minimum) or one (maximum) attosecond pulses



#### Attosecond science

## The fast show

### Extremely short laser pulses can illuminate electrons in motion

ON THE atomic scale, things move mind-bogglingly quickly. Electrons jump between orbits or escape the nucleus altogether in attoseconds—that is, million, million, millionths of a second. Indeed, one attosecond is to one second what one second is to the age of the universe. Seeing such acrobatics takes wit and ingenuity, but it is possible. Moreover, if such processes could be manipulated—and the early signs are that they can—then it would have applications in fields as far apart as computing and medicine.

A report just drafted by America's National Research Council, "Controlling the Quantum World", outlines how scientists might manipulate the inner workings of a molecule. A long-term workshop at the Kavli Institute for Theoretical Physics, part of the University of California, Santa Barbara, is also investigating how this might be achieved. And, at a conference held recently at the institute, Ferenc Krausz of the Max Planck Institute of Quantum Optics in Garching, Germany, and Marc Vrakking of the FOM Institute for Atomic and Molecular Physics in Amsterdam described one way that it could be done.

Lasers work by creating a chain reaction in which photons of light prompt the generation of further photons. These photons are emitted in bursts. Shortening each burst sufficiently is what makes atto-

second science possible. The two researchers employed what they call "high harmonic pulse generation" to create pulses a few hundred attoseconds long. They did this by using a laser that emits short pulses of light to drive a second laser that then emits even shorter pulses. In fact, the pulses are so rapid that they come close to the limit imposed by Heisenberg's famous uncertainty principle, which states that the precision of a time measurement is limited by the precision of a corresponding energy measurement.

#### Atto boys

Dr Krausz and Dr Vrakking fired their laser at a molecule of deuterium. Deuterium, also known as heavy hydrogen, is a simple molecule, consisting of two atomic nuclei and two electrons. The sample under investigation became positively charged because zapping it with the laser removed one of the electrons. The researchers found that the molecule then separated into a deuterium atom, consisting of a nucleus and an electron, and a deuterium ion, consisting of a nucleus.

Using conventional laser pulses causes atoms and ions to be ejected to the right and left at random. Using ultrafast laser pulses, though, makes the atoms fly off to the right and the ions to the left. The researchers were thus able, in effect, to con-

trol on which of the two deuterium atoms the electron resides at the end of their experiment. That is to say, they had separated the atoms from the ions.

Exactly how this works is complicated—not least because all of the atoms are interacting simultaneously with the laser and with each other. But the researchers think that the laser pushes the electron, which initially binds the two atoms together, back and forth between the two ions until, at some point, the distance between the two gets too large and it is no longer able to jump from one to the other.

The ability to manipulate electrons in this way is important because electron-sharing is essential to chemical bonding. Ultrafast lasers could thus be used to change the outcome of chemical reactions. Proponents point to possible applications in magnetic information-storage devices, which would lead to much more powerful computers. Other possibilities include the development of compact, portable x-ray lasers for medical imaging that needs to be done outside hospital radiology departments, and bright ultrafast x-ray lasers for use within those departments.

The motion of electrons is the fundamental basis of chemistry. Watching the steps in the dance of the electrons will help chemists work out why some atoms bind when others do not, why reactions take the time that they do, and why some molecules bend one way and not the other. Brighter x-ray lasers could also be used to reveal the atomic details of chemical catalysis or the way that light energy is absorbed and stored during photosynthesis, according to the National Research Council report. Knowing exactly how to capture sunlight and turn it into chemical energy would be a prize indeed. ■

#### Also in this section

72 Negative databases

72 Supernovas

73 Gene therapy and cancer

73 The virtues of cider

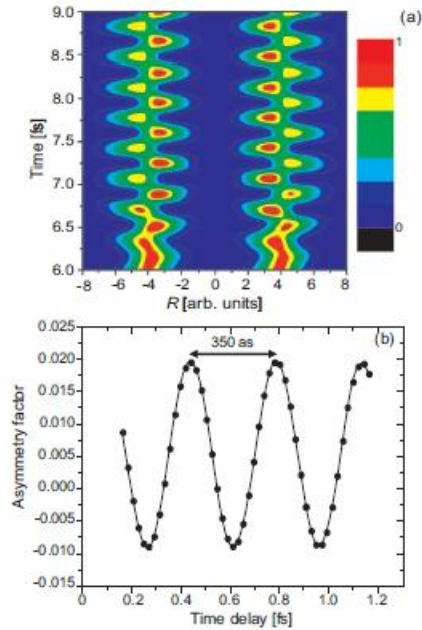


FIG. 53. (Color) Proposal for inducing attosecond electron wave-packet dynamics by a 0.8-fs, 115-nm VUV pump pulse in  $\text{H}_2^+$  and probing it with a time-delayed 0.1-fs, 20-nm XUV pulse (Bandrauk *et al.*, 2004). Both pulses are polarized parallel to the molecular axis. (a) Contour plot of the electron probability distribution along the molecular axis for an internuclear distance of eight atomic units vs pump-probe delay. (b) Asymmetry factor  $(P_- - P_+)/ (P_- + P_+)$  vs delay, where  $P_+$  and  $P_-$  represent the probability of observing the electron liberated by the XUV probe in the positive or negative direction (along the molecular axis), respectively. Adapted from Bandrauk *et al.*, 2004.

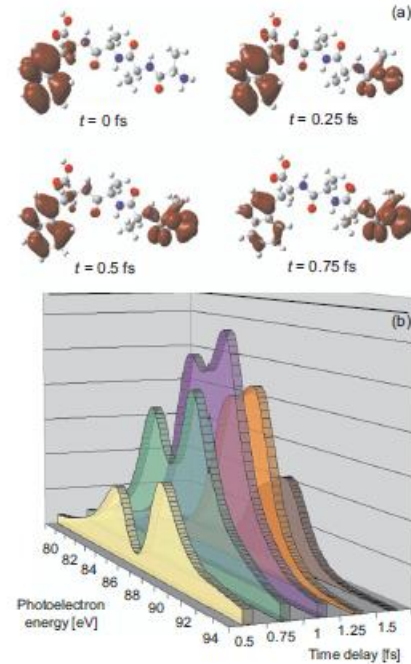


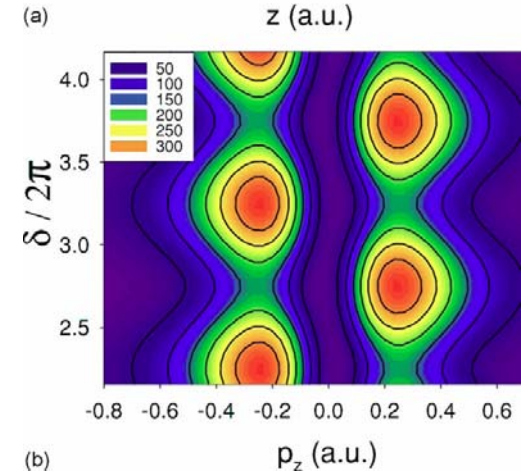
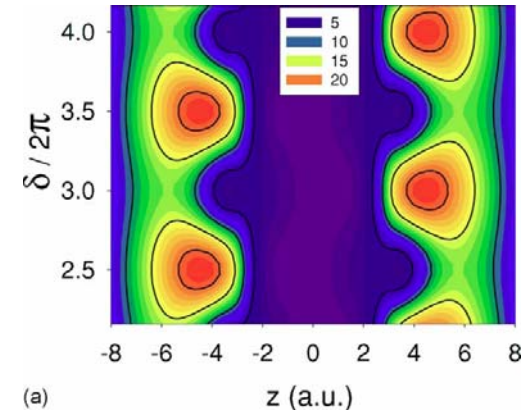
FIG. 54. (Color) Computed ultrafast positive charge (hole) migration in a tryptophane-terminated tetrapeptide (Remacle and Levine, 2006a, 2007). (a) The hole density shown in red indicates that the charge swings across the entire peptide from the aromatic amino acid on the left to the  $N$  end on the right within less than one femtosecond, following excitation of the electronic wave packet on an attosecond time scale. This hyperfast charge migration is proposed to be probed by measuring the kinetic energy distribution of photoelectrons released by a time-delayed sub-fs XUV pulse. (b) A series of such freeze-frame spectra calculated for a 250-as, 95-eV probe pulse at different pump-probe delays. From Remacle and Levine.

## Measuring electron wave packets

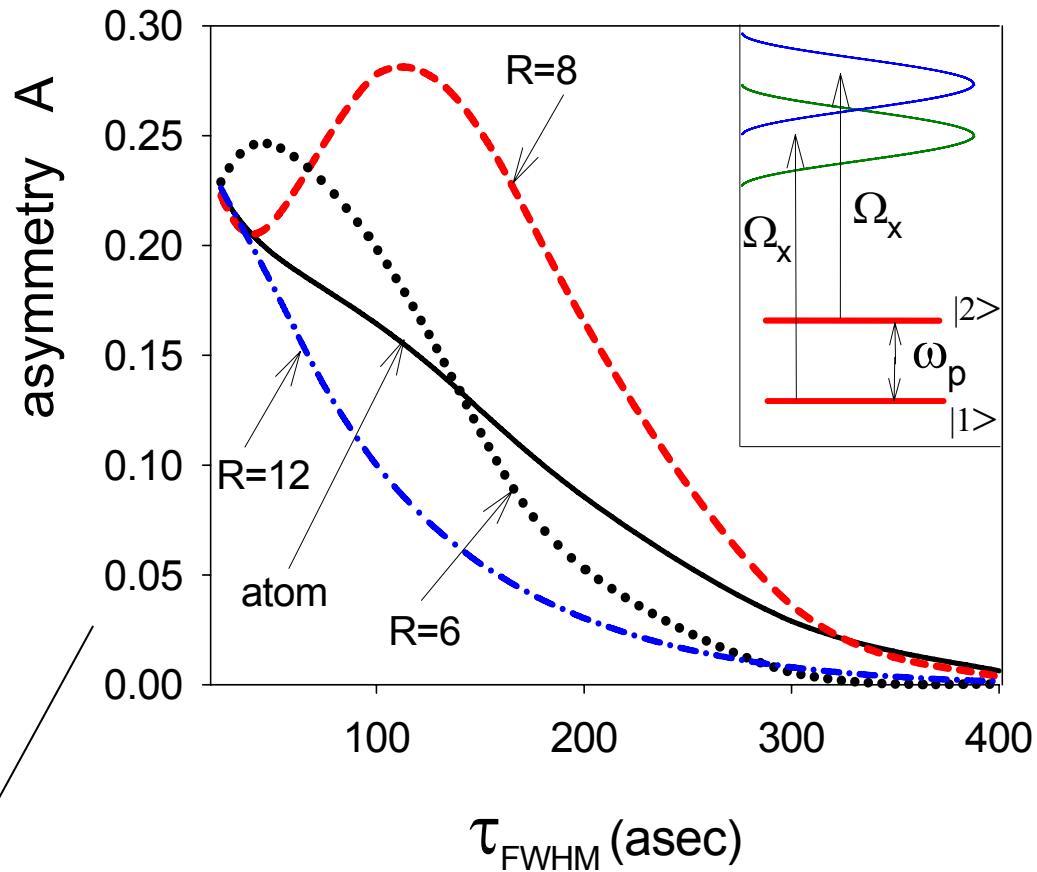
1. Attosecond pulses are fast enough to observe electron wave packets.
2. Electron wave packets are resolved through changes to the photo-electron spectrum as a function of pump-probe time delay.
3. The attosecond pulse projects the momentum distribution into the continuum.

Yudin et al, Phys Rev A 72, 51401(R) (2005)

J. Phys. B39, S409 (2006)

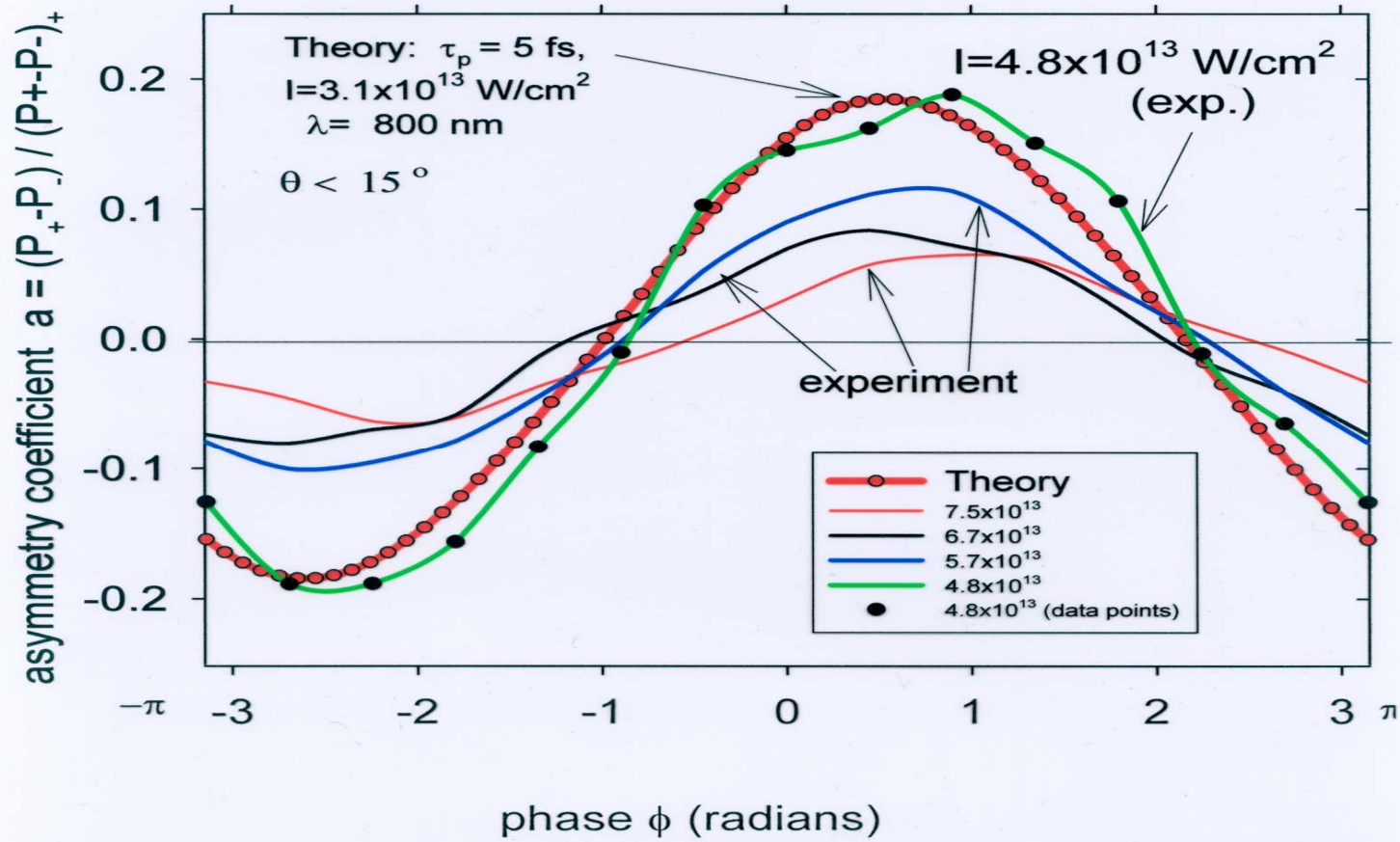


Atom:  $1s+2p$  and  $\diamond_g 1s + \diamond_u^* 2p$  in  $H_2^+$



no asymmetry in atomic  $1s + 2s$  and in molecular:  $\diamond_g 1s + \diamond_g^* 2s$ , but there asymmetry in  $\diamond_g 1s + \diamond_u^* 2s$

Experimental asymmetries (Garching).  
 F. Lindner, Ph.D. Thesis.  
 $\lambda=760$  nm,  $\tau_p=5$  fs .



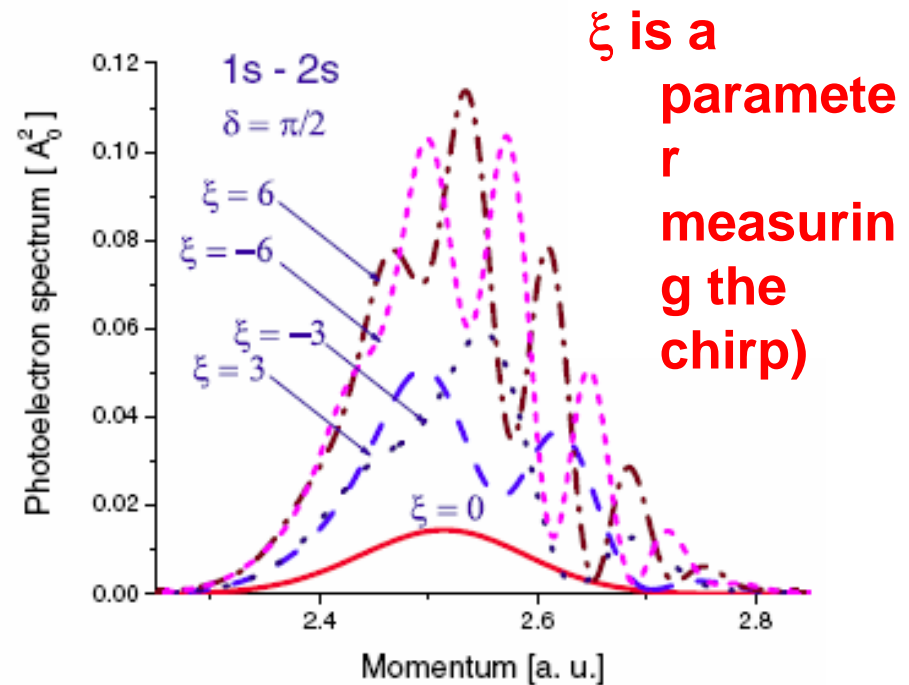
•Phys. Rev. A, 70, 013815 (2004)

•Opt. Lett. 29, 1557 (2004)



Chirped pulses (formed naturally with attosecond pulse technology) are as effective as transform limited pulses of the same bandwidth.

1. With a chirped pulse, all dynamic information is gained with only a single pump-probe time delay



# Attosecond photoionization of a coherent superposition of bound and dissociative molecular states: effect of nuclear motion

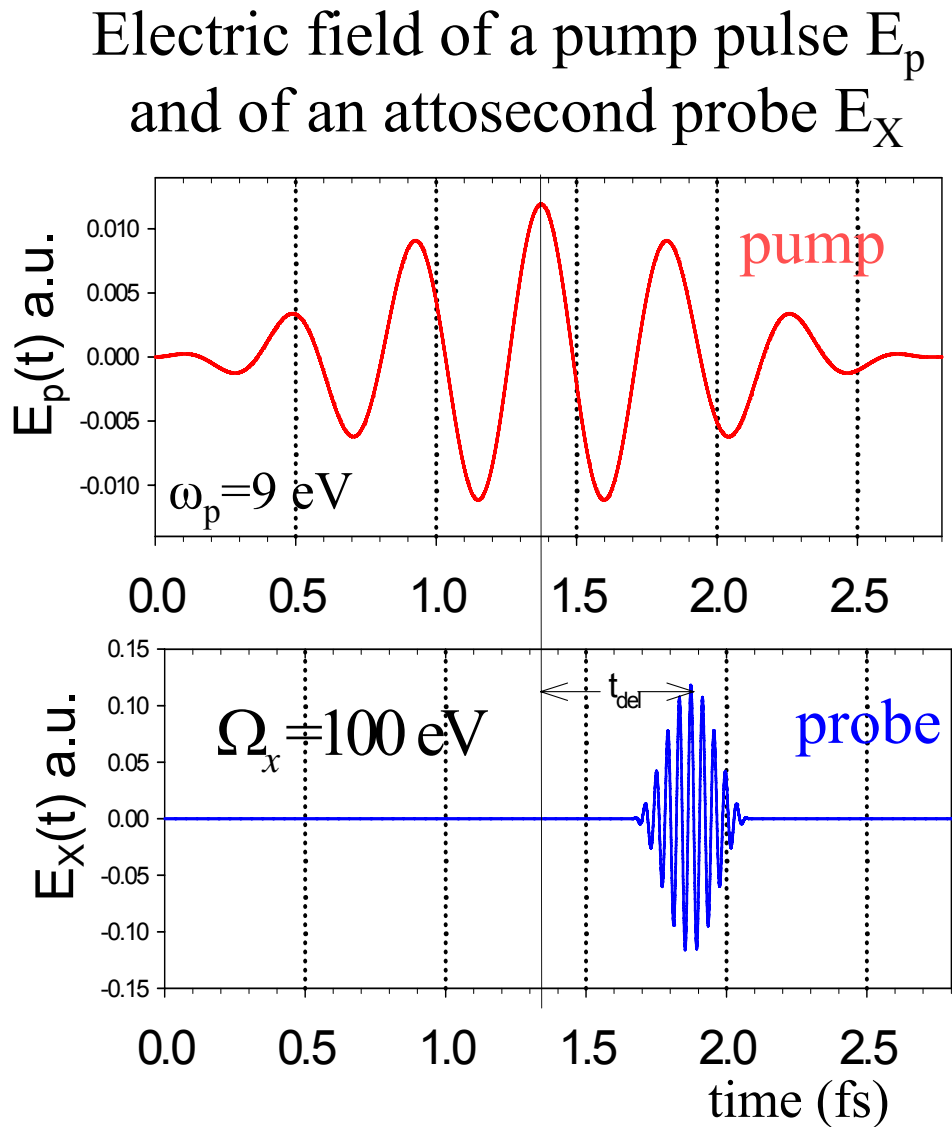
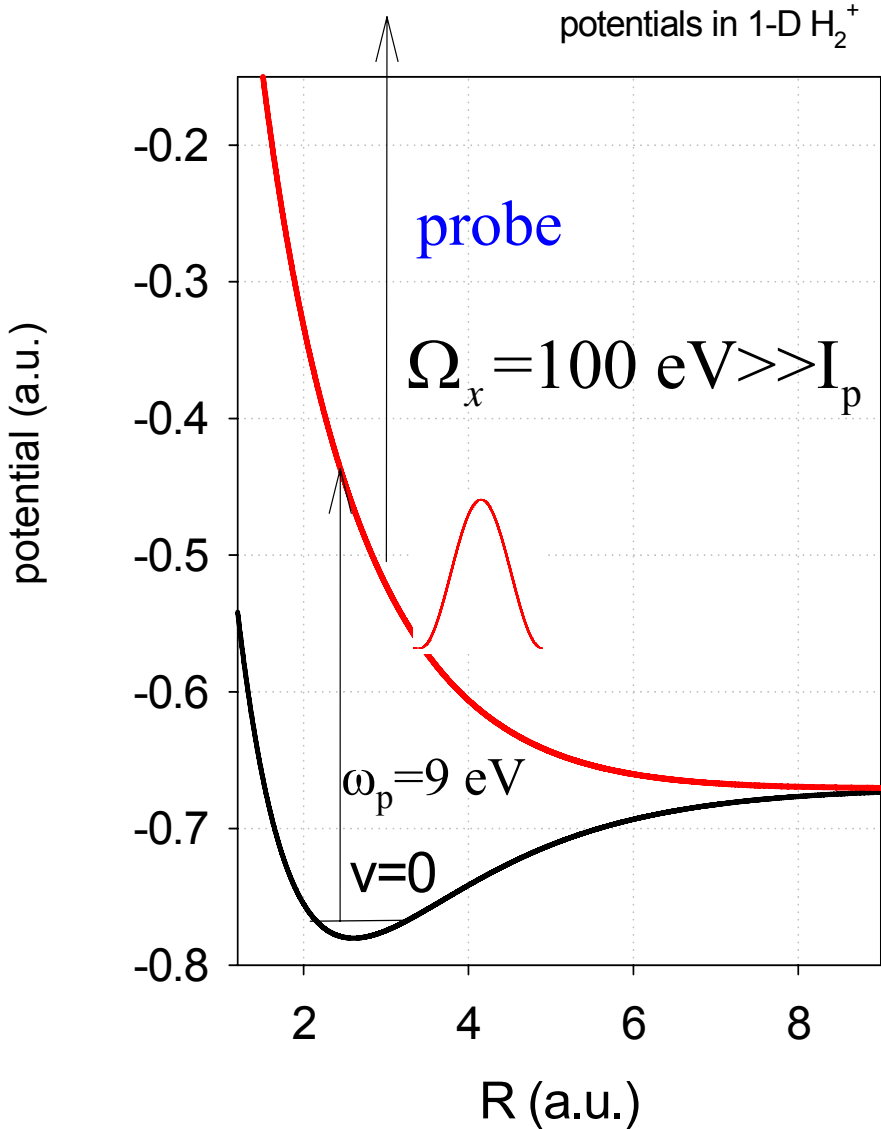
by

**André D. Bandrauk,**

**with S.Chelkowski, G.L. Yudin,**  
Université de Sherbrooke, Canada

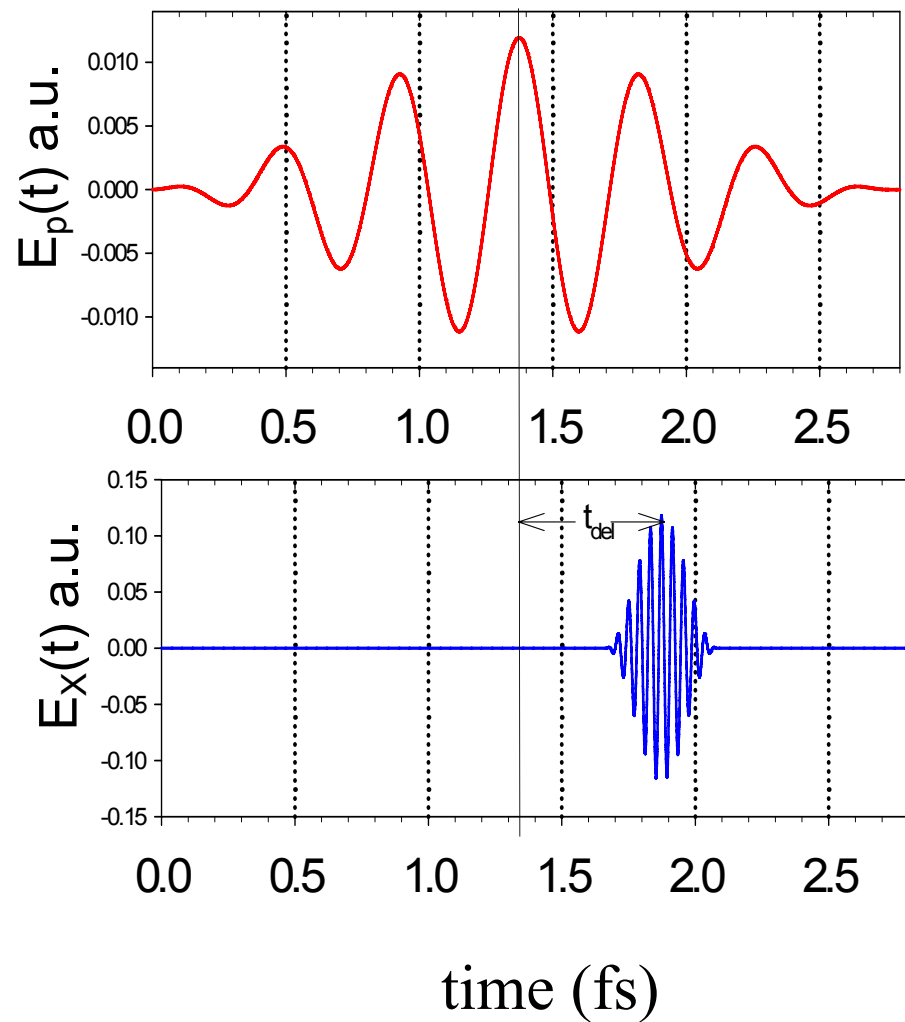
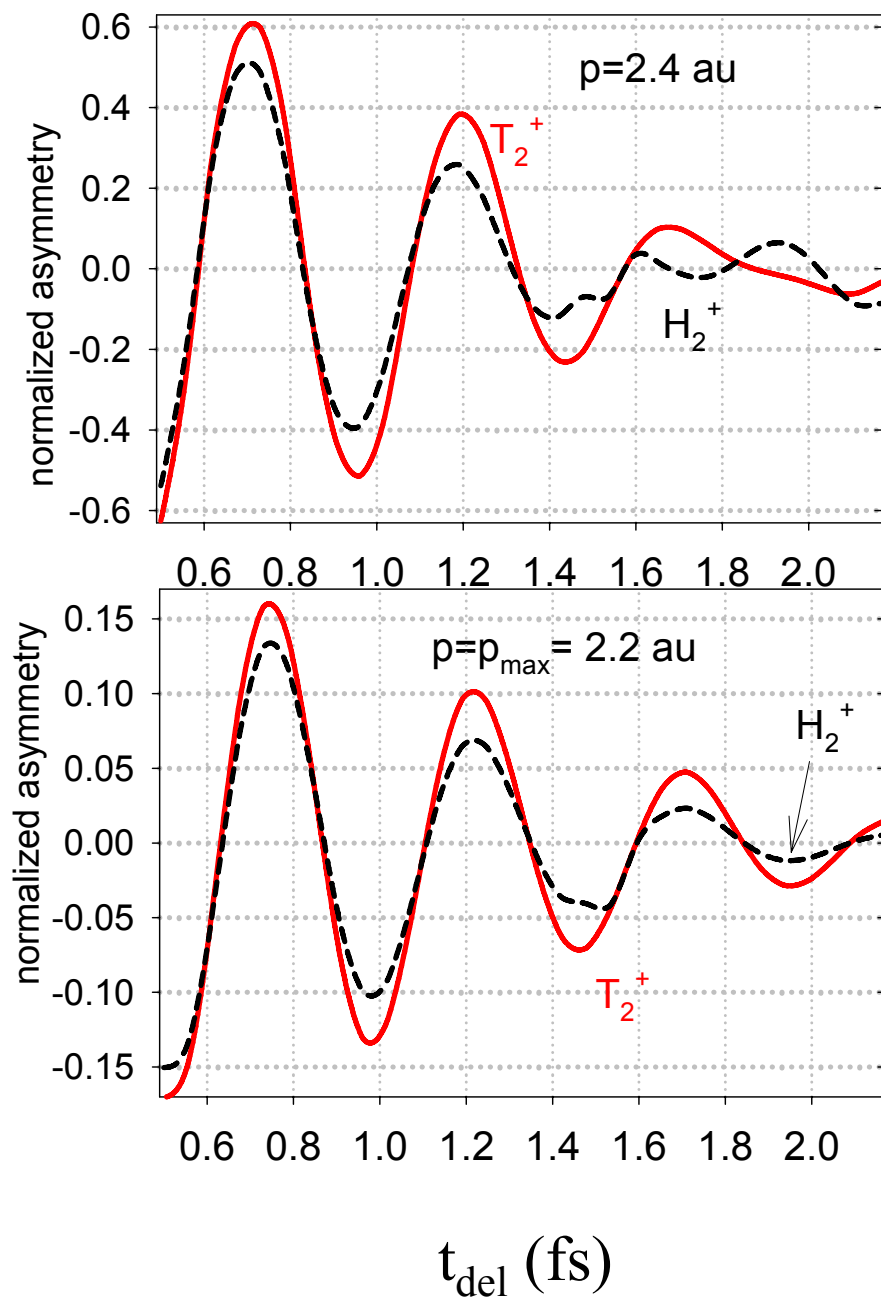
**P.B. Corkum (Ottawa),  
J. Manz (Berlin)**

to appear J Phys B 2009

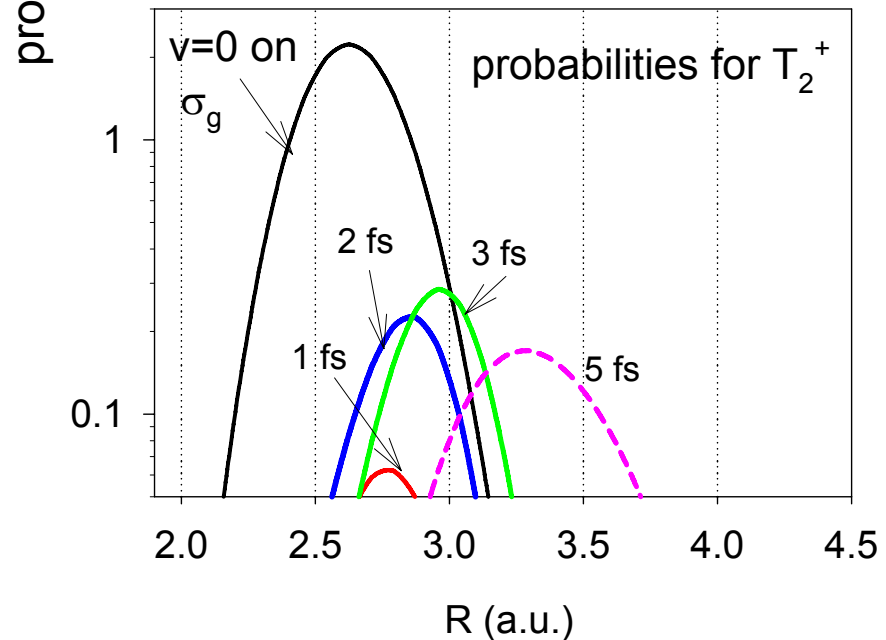
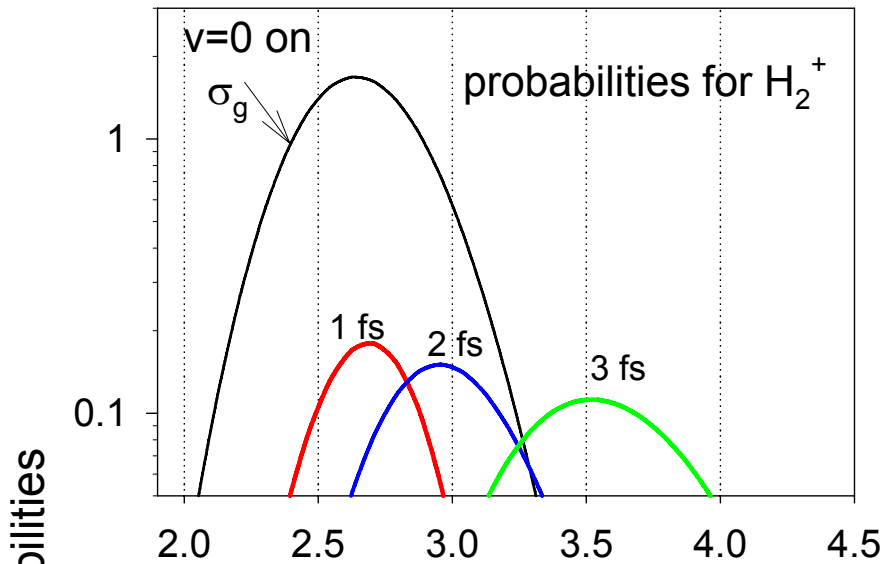


We solved the TDSE for a series of delays:  $t_{\text{del}} = 0.5 \text{ fs} + k T_1 / 8$ ,  
 $k=0,1,\dots$   $T_1 = 2\pi/\omega_p$ . We calculated the forward and backward)  
 photoelectron spectra  $S(p)$   $T_1/8 = 0.46 \text{ fs}$

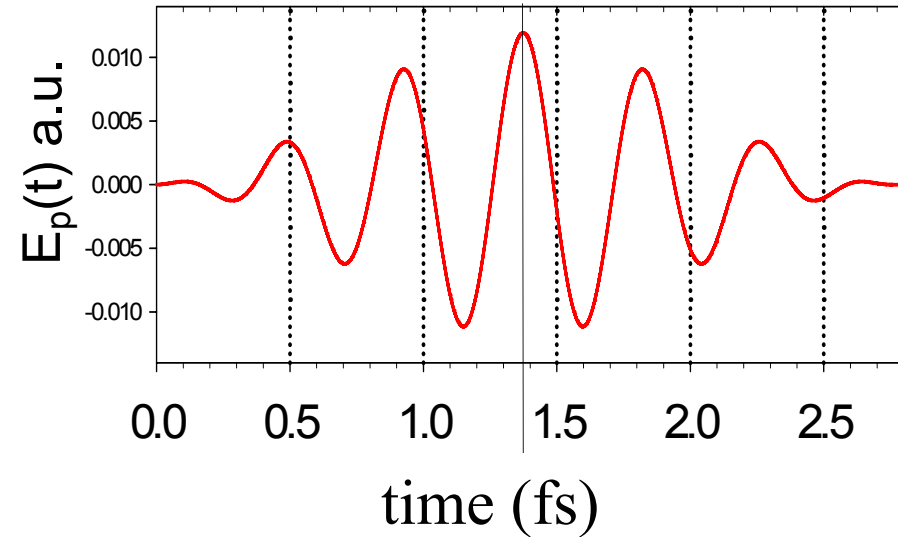
### Moving $H_2^+$ and $T_2^+$



$$\text{asymmetry} = \frac{S_{\text{forw.}}(p) - S_{\text{backw.}}(p)}{S_{\text{forw.}}(p) + S_{\text{backw.}}(p)}$$



Wave packet motion induced by the pump shown below:

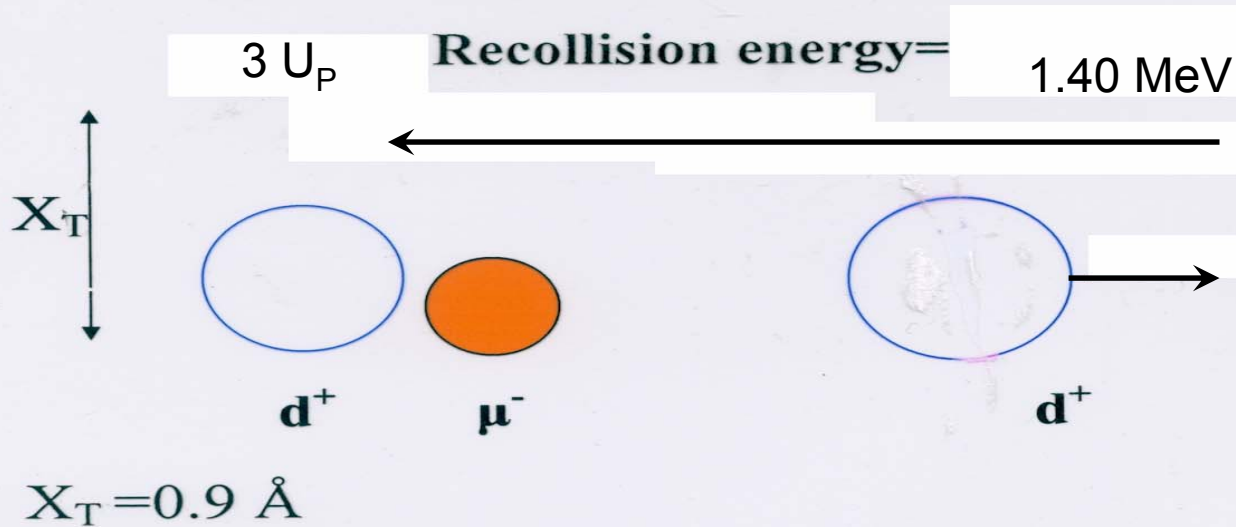


We show the initial  $v=0$  vibrational state and the dissociating packets on  $\sigma_u$ .

Conclusion: at  $t > 3$  fs ( $t_{del} > 1.5$  fs) we lose the overlap in  $H_2^+$ . This agrees with the attenuation seen in the previous slide

Decoherence?: see Zurek, PRD 47,488(1993)

**RECOLLISION OF  $d^+$  WITH A  $\mu d$  ATOM INITIATED BY A SUPER-INTENSE LASER**



**ELECTRIC FIELD  $E(t)$  OF THE LASER**

$$\lambda = 800 \text{ nm}$$

**THUS THE LASER CAN INITIATE**

**A NUCLEAR REACTION ,e.g:**

$$I - 3 \times 10^{22} \text{ W/cm}^2$$



or



# POTENTIALS OF $d-\mu-d$ IN DC ELECTRIC FIELD

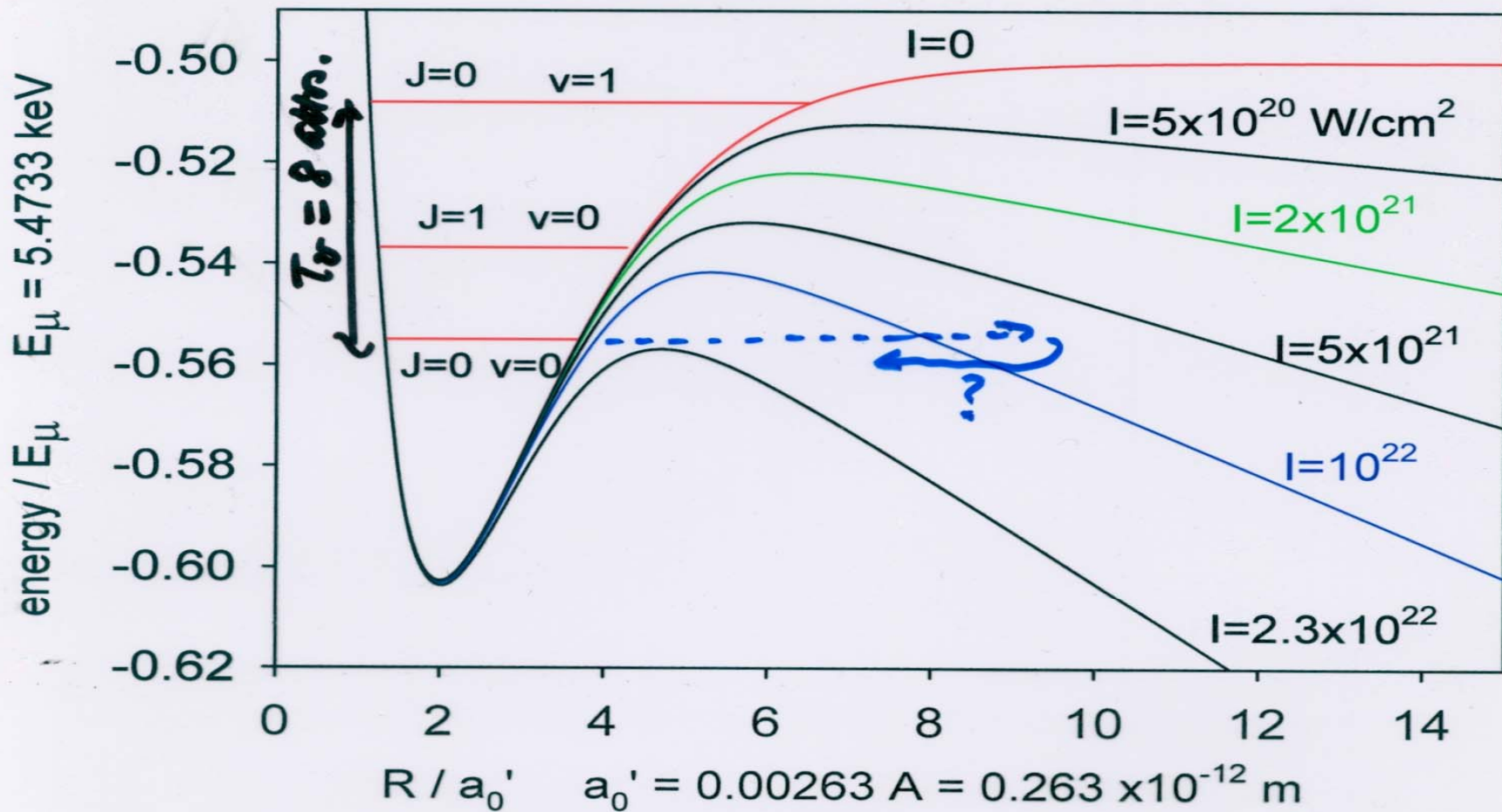


Fig.1

$\text{H}^+_2$  (Bond Softening / PH. Bucksbaum PR '90-92)

$\text{Ar}^{R2+}$  (Bond Softening / ADB (JCP 1981))

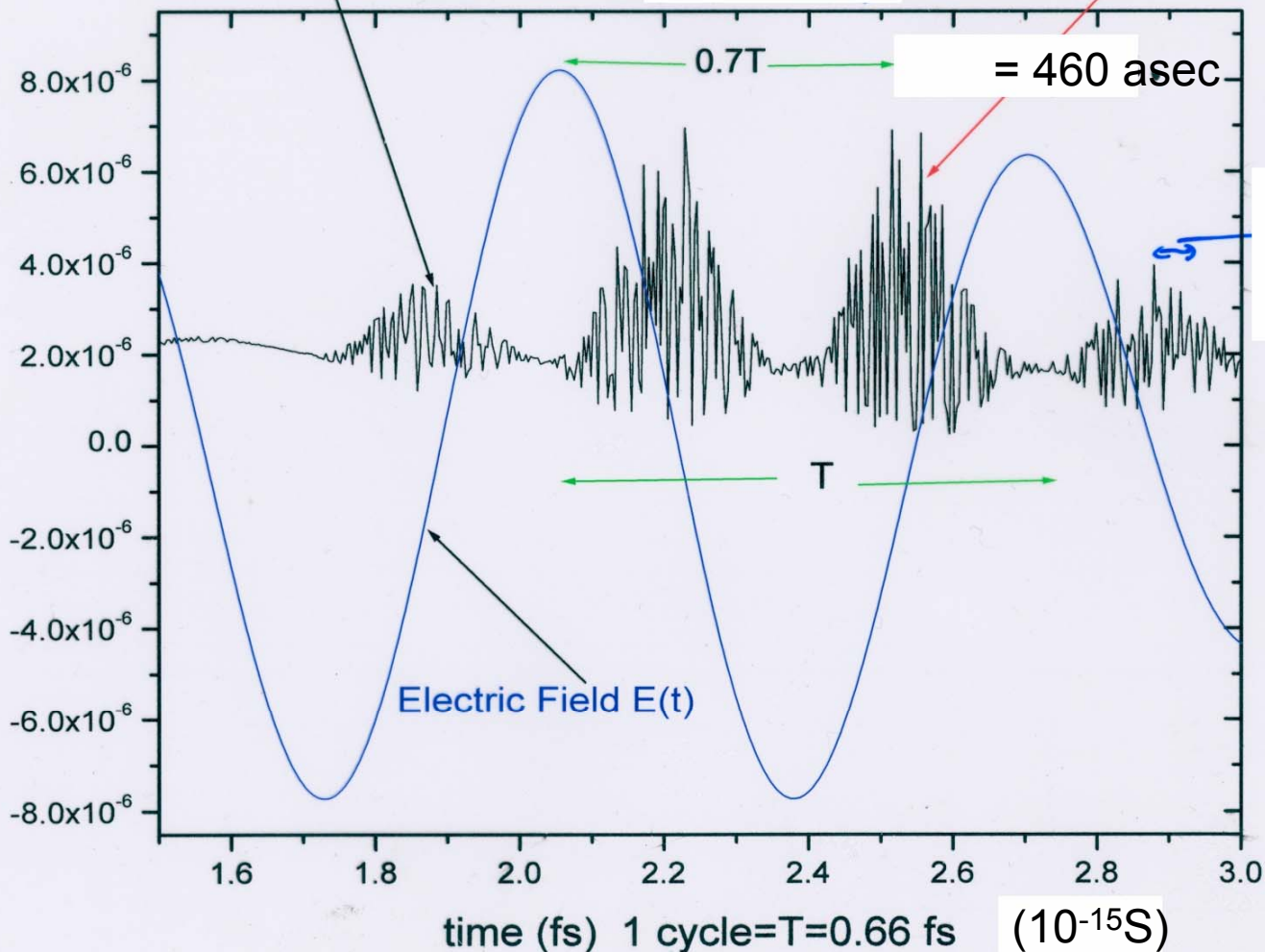
d- $\mu$ -d molecule dissociating in  
200 nm,  $I=10^{22}$  W/cm<sup>2</sup> laser field

deuterium returns back !

probability for  $R < 0.25 \mu$  un. ( $1 \mu$  un. = 0.0026 Angstrom)  
 $26 \times 10^{-14}$  m)

$E \sim 1/2$  MeV


Probabilities and the electric field adjusted to the scale





# Mathematical Problems

1. High order SOT
2. Multiscale time frequency analysis
3. Infinite D Optimal Control theory
4. High order NLS
5. Relativistic QM
6. Molecular movies  
(Dynamic Imaging of Electrons-Nuclei)

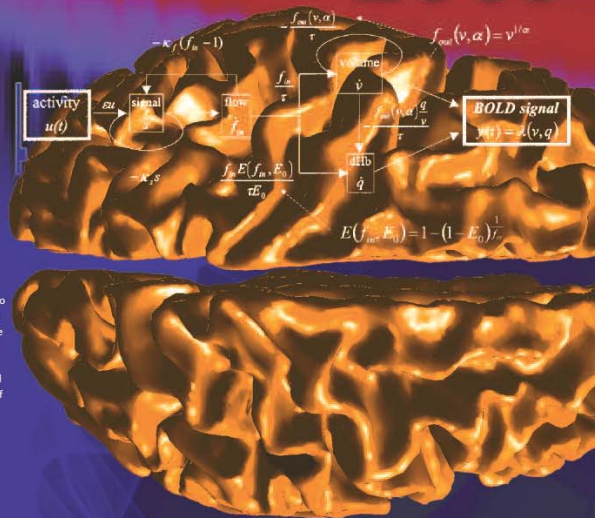
$$i \hbar \frac{\partial \Psi}{\partial t} = H \Psi$$


THEMATIC SEMESTER

# Mathematical Problems in Imaging Science: From the Neuronal to the Quantum World

Centre de recherches mathématiques  
Montréal, Canada

August  
December **2009**



During the last 20 years, biomedical and biomolecular imaging has played an increasing role as it becomes more and more accurate both in time and space. In particular, neuroimaging has benefited from various advanced techniques and methodologies where applied mathematics have been able to contribute in a very significant way. The first three workshops will explore neuroimaging along three themes where mathematics have played a major role: the neuronal and vascular modulation of the cerebral functional activity, the resolution of inverse problems in non-invasive neuroimaging and the sparse representations of signals. The fourth workshop will address mathematical problems arising from a revolution in molecular imaging via advanced laser technology: the possibility of imaging and thus controlling molecular dynamics at spatio-temporal dimensions down into the quantum world of the electron. This workshop is a continuation of previous CRM workshops on quantum control and highdimension PDEs, dealing with mathematical issues in describing quantum dynamics.

## SCIENTIFIC COMMITTEE

S. Baillet (Medical College of Wisconsin), A.D. Bandaru (Sherbrooke, CRM),  
H. Benali (CHU Hôpital Sainte-Justine, CRM), C. Groves (McGill), S. Jaffard (Paris VII),  
C. Le Bouc (CRMCS), D.P.O. Li (Ecole Polytechnique de Montréal), CRM,  
J.-M. Lina (Ecole de technologie supérieure, CRM), B. Schneider (NSF).

## ORGANIZING COMMITTEE

S. Baillet (Medical College of Wisconsin),  
A.D. Bandaru (Sherbrooke, CRM),  
H. Benali (CHU Hôpital Sainte-Justine, CRM),  
C. Groves (McGill),  
T. Huppert (Pittsburgh),  
M.Y. Nazari (MRC-CHC, Ottawa, Imperial College),  
S. Jaffard (Ecole Polytechnique de Montréal, CRM),  
F. Lesage (Ecole de technologie supérieure, CRM),  
J.-M. Lina (Ecole de technologie supérieure, CRM).

## AISENSTADT CHAIRS

Stéphane Mallat (Ecole Polytechnique, Paris; Courant Institute, NY),  
September 2009  
Claude Le Bouc (CRMCS, Ecole Nationale des Ponts et Chaussées)  
October 2009

## WORKSHOPS

### Brain Activity Modeling: From Fine to Coarse Scale

August 17-22, 2009

Organizers: H. Benali (CHU Hôpital Sainte-Justine, CRM), T. Huppert (Pittsburgh), F. Lesage (Ecole Polytechnique de Montréal, CRM)

The preliminary list of invited speakers includes: R. Barbot (UC San Diego),  
D. Boas (Harvard Medical School), S. Hamel (McGill), T. Huppert (Pittsburgh),  
R. Jolani (Zürich), J. Biera (Tokyo), Y. Zheng (Sheffield)

### Inverse Problems in Brain Imaging and Multimodal Fusion

August 24-29, 2009

Organizers: S. Baillet (Medical College of Wisconsin), C. Groves (McGill),  
J.-M. Lina (Ecole de technologie supérieure, CRM)

The preliminary list of invited speakers includes: S. Baillet (Medical College of Wisconsin), J. Daunizeau (VU Medical Center Amsterdam),  
J. De Munck (VU Medical Center Amsterdam), C. Groves (McGill),  
M. Hamalainen (M. Martinos Center for Biomedical Imaging, Boston),  
J. Mosher (Episcopal Center, Cleveland Clinic), J. Biera (Tokyo),  
H. Sapiro (McGill Center, Erlangen), N. Trujillo-Barrios (Cuban Center for Neurosciences)

### Dictionary of Atoms: New Trends in Advanced Signal Processing in Functional Brain Imaging

September 14-17, 2009

Organizers: S. Jaffard (Paris VII), F. Lesage (Ecole Polytechnique de Montréal), CRM,  
J.-M. Lina (Ecole de technologie supérieure, CRM)

The preliminary list of invited speakers includes: R. Barankin (Drexel, C. Deser (INSERM),  
M. Clerc (IRISA, Sophia Antipolis), A. Delorme (CNRS, San Diego), R. De Vries (South Carolina),  
R. Grunwald (MCA, S. Jaffard (Paris VII), G. Mallat (Ecole Polytechnique Paris),  
D. Van de Ville (EPFL), P. Valdes-Sosa (Cuban Center for Neurosciences), F. Wendling (INSERM)

### Quantum Dynamic Imaging

October 19-23, 2009

Organizers: A.D. Bandaru (Sherbrooke, CRM),  
M. Y. Nazari (MRC-CHC, Ottawa, Imperial College)

The preliminary list of invited speakers includes: A. Becker (Colorado),  
T. Blakes (Ottawa), K. Bartsch (Duke), T. Carrington (Queens),  
A. Emmanouilidou (Massachusetts), C.H. Kenton (M.D. Heidelberg),  
H. Kono (Tohoku, C.D. Lin (Kansas State), E. Lorin (Ontario University  
of Technology), A. Mazaoui (Paris VII), W. McCurdy (Lawrence Berkeley National Laboratory),  
V. McKoy (Czechia), J. Manz (FU Berlin), T.T. Nguyen Dang (Laval), R. Santra (Argonne National  
Laboratory), B.J. Schneider (NSF), G. Smerina (M.D. Berlin), A. Storz (Warsaw),  
K. Takahata (Tokyo), K. Taylor (Queens, Belfast), J. Terjeson (London), T. Ueber (Georgia Tech)

## FINANCIAL SUPPORT

Support is available for visitors, graduate students and postdoctoral fellows attending the various events. All requests must be accompanied by a reference. Furthermore, graduate students are asked to send a letter of recommendation from their research supervisor.

Please send your application for financial aid to:

Scientific Activities  
Centre de recherches mathématiques  
Université de Montréal  
C.P. 6128, Succursale Centre-ville  
Montréal (Québec)  
CANADA H3C 3J7  
Fax: 514-343-2254  
E-mail: activites@CRM.UMontreal.CA

This thematic program is funded by:

NSERC (Canada)  
FQRNT (Québec)  
Université de Montréal (where the CRM is located)  
MRC/CIHR (where the CRM is located)  
Université Laval  
Université de Québec à Montréal  
Concordia University  
Université Laval  
University of Ottawa  
Université de Sherbrooke

Funding is also expected from MITACS (Canada), the CRI (Canada), and the NSF (USA).

Because of limited space, those interested should register as soon as possible.

[www.crm.math.ca/Imaging2009](http://www.crm.math.ca/Imaging2009)

## Tracking Electrons

### Attosecond science opens the door to real-time observation and control of electron dynamics

Jyllian Kemsley

TEN YEARS AGO, Ahmed H. Zewail won the Nobel Prize for using femtosecond spectroscopy to study atomic motions during chemical reactions. Emerging now from Zewail's pioneering work is the ability to use femtosecond laser pulses to monitor attosecond-scale electron dynamics, which was the focus of a Division of Physical Chemistry symposium on attosecond science at the American Chemical Society national meeting in Salt Lake City last month.

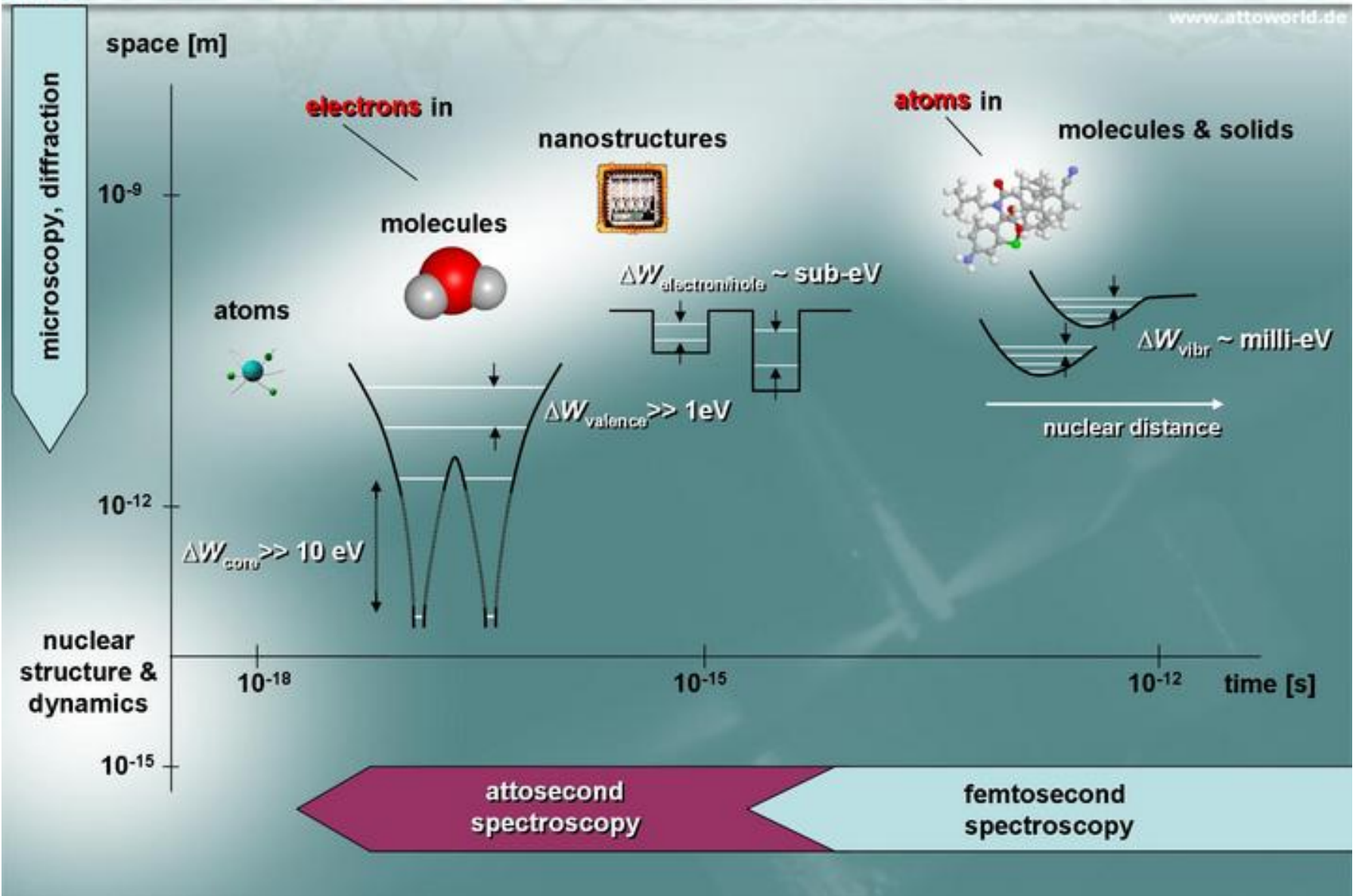
"There's a whole class of processes associated with electron dynamics that occur at a femtosecond timescale or less," Daniel M. Neumark, a chemistry professor at the University of California, Berkeley, said at the meeting. "These are electron dynamics processes that don't require nuclear motion. To probe them you need attosecond-scale pulses."



Gary Larson © 2004

**ULTRAFAS** A cryostat contains a cooled Ti:sapphire laser amplifier crystal that is used to generate high-power femtosecond pulses for attosecond experiments.

# structure and dynamics in the microcosm



# Quantum mechanics for plants

Graham R. Fleming and Gregory D. Scholes

To what extent do photosynthetic organisms use quantum mechanics to optimize the capture and distribution of light? Answers are emerging from the examination of energy transfer at the submolecular scale.

The first law of photosynthetic economics is: "A photon saved is a photon earned." Research into the factors behind this principle has been burgeoning, and has recently culminated in a paper in *Physical Review Letters* by Jang *et al.*<sup>1</sup> in which the authors look at photosynthetic energy transfer at the quantum level.

Plants use solar antennae to capture incident photons and transmit the excitation energy to reaction centres, where it is used to initiate the primary electron transfer reactions of photosynthesis. These antennae are one of nature's supreme examples of nanoscale engineering, and are constructed from specialized light-harvesting complexes formed of proteins that bind chlorophylls and carotenoids. Photon collection involves up to several hundred light-absorbing molecules, or chromophores. Hundreds of energy-transfer steps over a hierarchy of time scales and distances, which often occur with near-perfect efficiency<sup>2</sup>, are therefore required to collect and trap solar energy.

More than 50 years ago, Theodore Förster described a method for calculating the rate of energy transfer between molecules from the overlap of the donor molecule's fluorescence spectrum and the acceptor molecule's absorption spectrum<sup>34</sup>. The theory has had an enormous impact on biology, chemistry and physics. Collectively, high-resolution structural models, ultrafast spectroscopy and quantum chemical calculations have helped to expose the complex and, in some cases, subtle relationships between structure and light-harvesting in photosynthetic systems. Indeed, it has turned out that there are only a

few cases in which the energy transfer within photosynthetic light-harvesting complexes can be correctly characterized by conventional Förster theory. Moreover, the realization that the concepts elucidated during the study of light-harvesting proteins are general

chromophoric assemblies.

To understand the dynamics of light-harvesting and light-trapping in photosynthesis, certain design features must be taken into account. For example, the distances between the molecules are often smaller than the overall size of each molecule. In this confined geometry, energy transfer is governed by how the donor 'sees' the acceptor on the submolecular scale at which the fine differences in the shape of the wavefunctions between the ground and excited states at the donor-acceptor junction become significant (Fig. 1). At this level of spatial confinement, transitions and energy levels that would be ineffective, or even inoperative, in

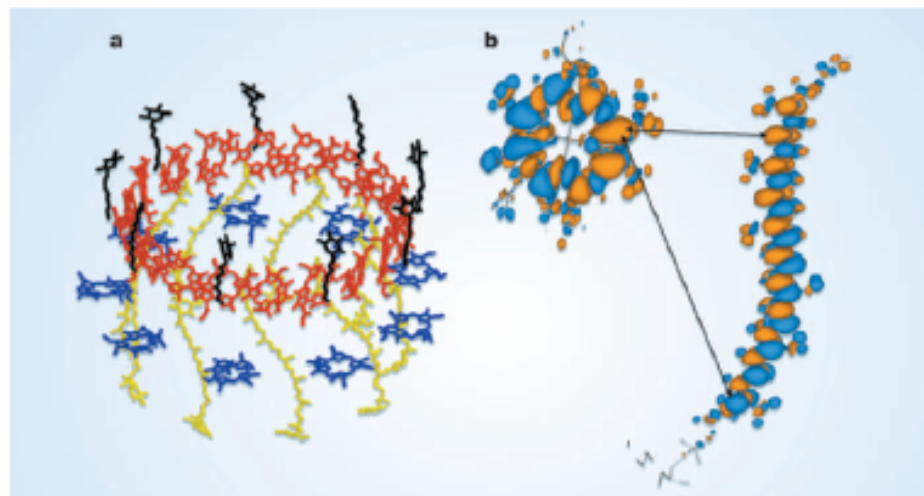
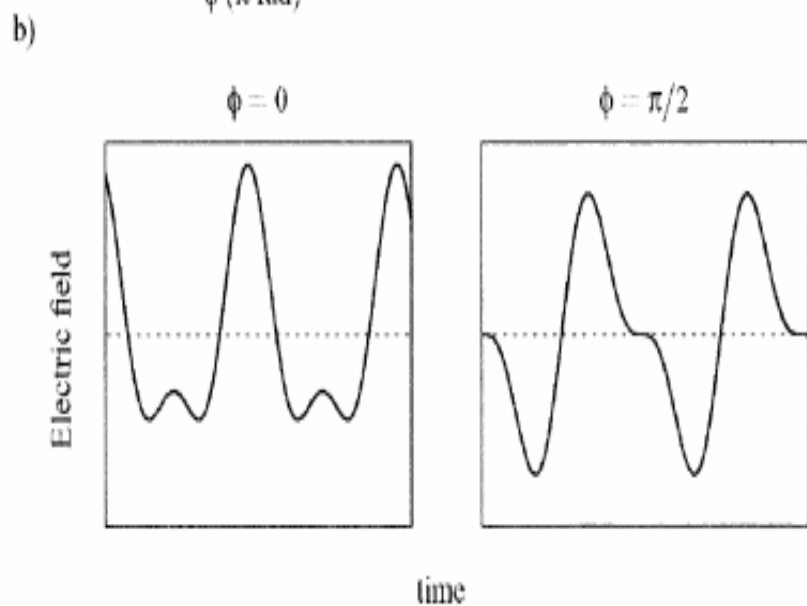
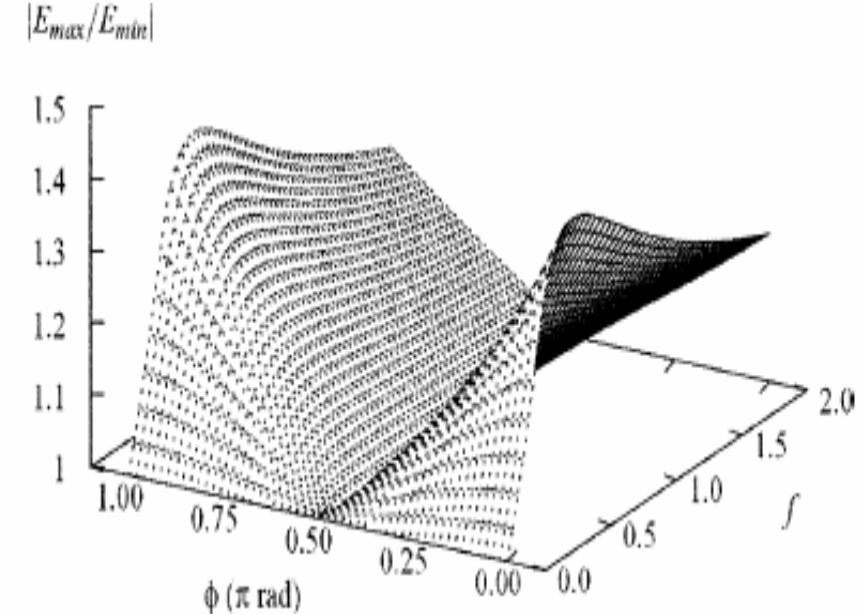
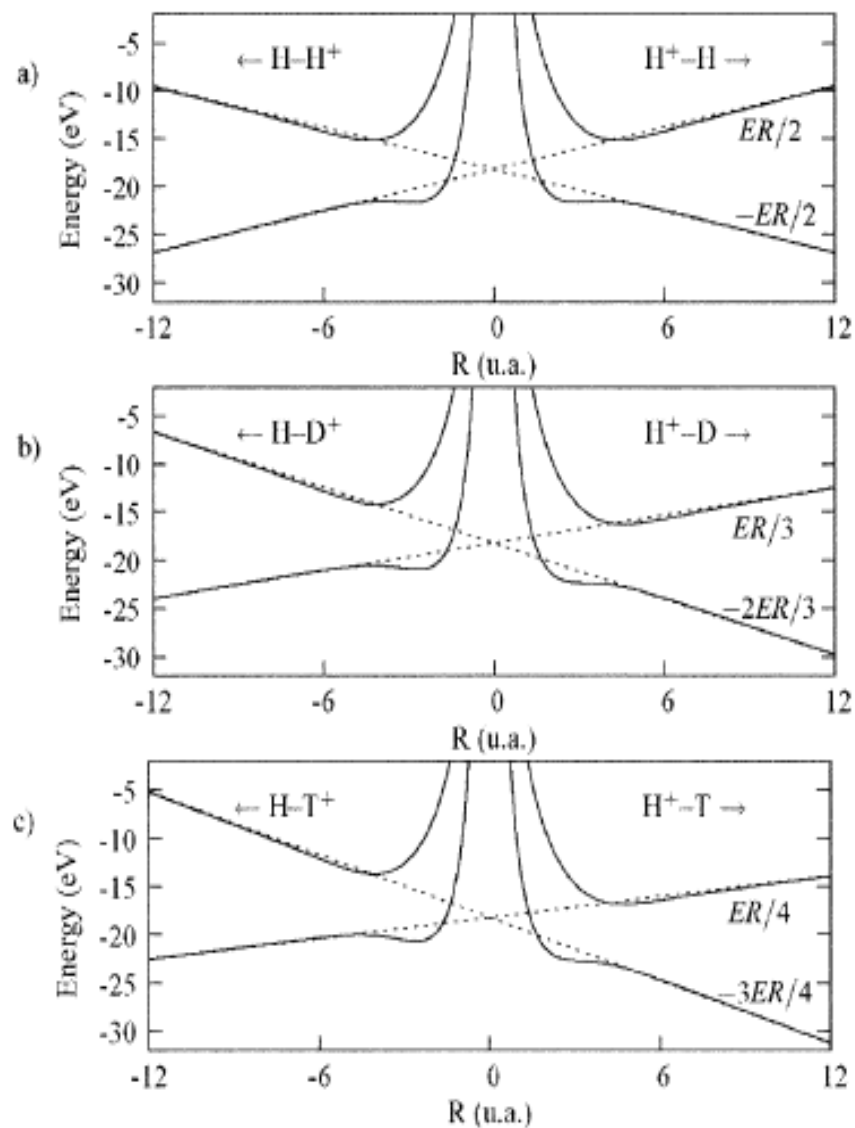


Figure 1 Designs for energy transfer. a, Chromophores in a model of light-harvesting complex (LH) 2 from the bacterium *Rhodospseudomonas acidophila* (Fig. 2), radius 3.4 nm. B800 bacteriochlorophyll molecules (blue) are widely spaced and constitute simple donors, but the B850 molecules (red) interact strongly and constitute a complex acceptor in a confined geometry. Through such interactions between molecules, photosynthetic organisms employ quantum mechanics to funnel absorbed photons to the reaction centre. On time scales of less than 1 picosecond, energy flows from the 800-nm-absorbing B800 molecules to the 850-nm-absorbing B850 molecules, and from the carotenoids (yellow) to both B800 and B850. b, A real-space picture of electronic interactions between molecules on a submolecular scale, as seen in the transition densities of LH2 bacteriochlorophyll (left) and carotenoid (right) molecules calculated from ground- and excited-state wavefunctions. The different colours represent the sign of the electron density. Instead of one average separation between donor and acceptor defining the energy transfer rate, as in Förster theory, there are clearly many length scales (examples arrowed) over which the various parts of the donor and acceptor electron densities interact.



**Figure 2.** Total field  $E(t)$  (eq 3): (a) Ratio of maximum,  $E_{\max}$  and minimum  $E_{\min}$  field amplitudes as a function of phase  $\phi$  and relative amplitude  $f$ ; (b) ratio  $E(t)/E_0$  for phases  $\phi = 0$  and  $\phi = \pi/2$ ,  $I_0 = 4.4 \times 10^{13}$  W/cm<sup>2</sup>,  $f = 0.5$ .



**Figure 3.** Molecular potentials for (a)  $H_2^+$ , (b)  $HD^+$ , and (c)  $HT^+$  in a static electric field corresponding to the peak strength  $E_{\max}$  of a  $10^{14}$  W/cm<sup>2</sup> laser radiation. The figures show both orientations for the field-aligned molecules, so that the positive coordinates correspond to the proton being upfield ( $H_2^+$ ,  $DH^+$ ,  $TH^+$ ), while the negative coordinates show the potentials for the orientation with the proton downfield ( $H_2^+$ ,  $HD^+$ ,  $HT^+$ ).

We enumerate the pairs of integrators with second, third and fourth-order accuracies for later numerical comparison:

$$S_2^A = e^{\gamma\lambda A} e^{\lambda B} e^{\gamma^* \lambda A} + (\mathcal{O}(\lambda^3)), \quad \gamma = \frac{1}{2}, \quad (18)$$

$$S_2^B = e^{\gamma\lambda B} e^{\lambda A} e^{\gamma^* \lambda B} + (\mathcal{O}(\lambda^3)), \quad \gamma = \frac{1}{2}, \quad (19)$$

$$S_3^B = e^{\gamma\lambda B/2} e^{\gamma\lambda A} e^{\lambda B/2} e^{\gamma^* \lambda A} e^{\gamma^* \lambda B/2} + (\mathcal{O}(\lambda^4)),$$

$$\gamma = \frac{1}{2} \left( 1 \pm \frac{i}{\sqrt{3}} \right), \quad (20)$$

$$S_3^A = \frac{1}{2} (e^{\gamma\lambda B} e^{\lambda A} e^{\gamma^* \lambda B} + e^{\gamma\lambda A} e^{\lambda B} e^{\gamma^* \lambda A}) + (\mathcal{O}(\lambda^4)),$$

$$\gamma = \frac{1}{2} \left( 1 \pm \frac{i}{\sqrt{3}} \right), \quad (21)$$

$$S_4^B = e^{\gamma\lambda B/2} e^{\gamma\lambda A} e^{(1-\gamma)\lambda B/2} e^{(1-2\gamma)\lambda A} e^{(1-\gamma)\lambda B/2} e^{\gamma\lambda A} e^{\gamma\lambda B/2}$$

$$+ (\mathcal{O}(\lambda^5)), \quad \gamma = (2 - 2^{1/3})^{-1}, \quad (22)$$

$$S_4^A = \frac{1}{2} (e^{\gamma\lambda B/2} e^{\lambda A/2} e^{\gamma^* \lambda B} e^{\lambda A/2} e^{\gamma\lambda B/2} + e^{\gamma\lambda A/2} e^{\lambda B/2} e^{\gamma^* \lambda A} e^{\lambda B/2} e^{\gamma\lambda A/2})$$

$$+ (\mathcal{O}(\lambda^5)), \quad \gamma = \frac{1}{2} \pm \frac{i}{2\sqrt{3}}. \quad (23)$$

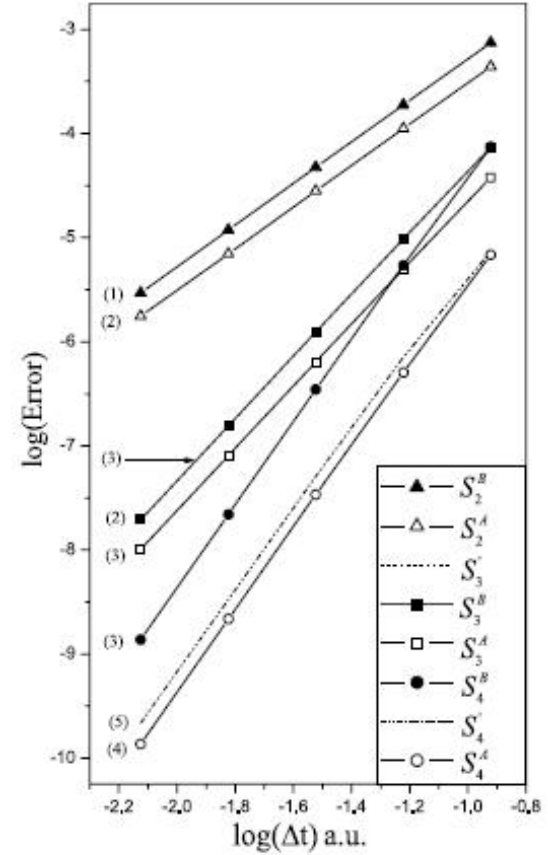


Fig. 1. Test of convergence for ground state of  $H_2^+$  (Eqs. 25 and 26).  $m$  corresponds to number of FFT's,  $N_{\text{FFT}}$ .

# Japanese connection

